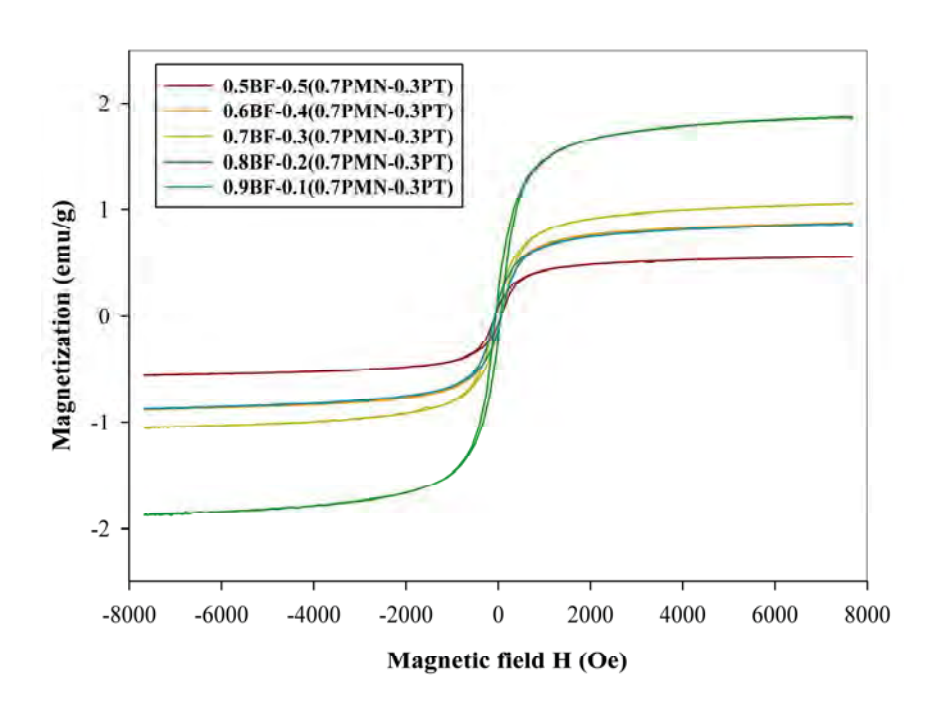
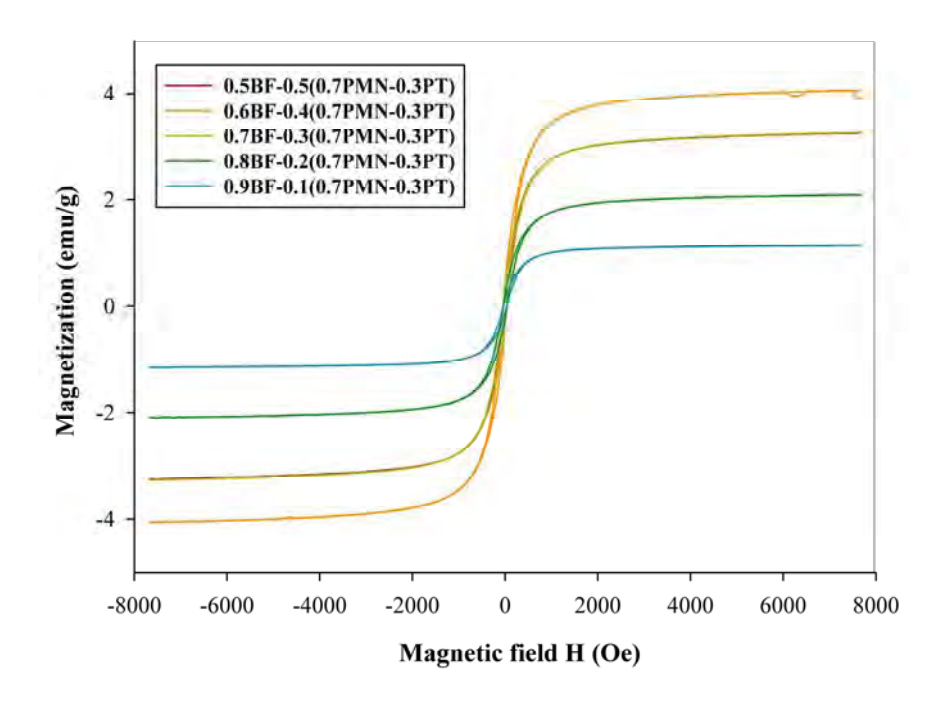
# 4.3.8 ผลการตรวจสอบ M–H hysteresis loops ของเซรามิกมัลติเฟร์โรอิกนาโนคอมโพสิตในระบบ (1-x)BF-x(0.7PMN-0.3PT)

จากการนำเซรามิกมัลติเฟร์โรอิกนาโนคอมโพสิตในระบบ (1-x)BF-x(0.7PMN-0.3PT) ที่ เตรียมได้จากการเผาซินเตอร์ที่อุณหภูมิ 800 และ 900 °ซ มาตรวจสอบ M–H hysteresis loops โดย ใช้สนามแม่เหล็กประมาณ -8  $\leq H_{\rm c} \leq$  8 kOe พบว่าจะได้ผลดังแสดงในรูป 1.36 และ 1.37 ซึ่ง M–H hysteresis loops ที่ได้แสดงพฤติกรรมทางแม่เหล็กคล้ายคลึงกับที่พบในระบบ (1-x)BF-xPMN และ (1-x)BF-x(0.9PMN-0.1PT) คือมีพฤติกรรมแบบเฟร์โรแมกเนติก โดยมีค่า saturation magnetization ( $M_{\rm s}$ ) สูงสุด เมื่อ x=20 และ 40 %wt เมื่อเผาที่ 800 และ 900 °ซ ตามลำดับ และค่า  $M_{\rm s}$  ที่วัดได้ก็มี ค่าสูงกว่าเซรามิก BF ที่มีค่าประมาณ 0.2 emu/g และเห็นได้ว่าค่า  $M_{\rm s}$  ที่วัดได้จะลดลงเมื่อปริมาณ 0.7PMN-0.3PT เพิ่มขึ้น ซึ่งแตกต่างจากค่า  $M_{\rm s}$  ที่วัดได้จากเซรามิกที่ผ่านการเผาที่อุณหภูมิ 900 °ซ เนื่องจากค่า  $M_{\rm s}$  ที่วัดได้จากเซรามิกชุดที่สองนี้จะมีค่า  $M_{\rm s}$  เพิ่มขึ้นเมื่อปริมาณ 0.7PMN-0.3PT เพิ่มขึ้น



รูป **1.36** M–H hysteresis loops ของเซรามิกมัลติเฟร์โรอิกนาโนคอมโพสิตในระบบ BF-(0.7PMN-0.3PT) เมื่อผ่านการเผาซินเตอร์ที่อุณหภูมิ 800 °ซ นาน 2 ชั่วโมง



รู**ป 1.37** M–H hysteresis loops ของเซรามิกมัลติเฟร์โรอิกนาโนคอมโพสิตในระบบ BF-(0.7PMN-0.3PT) เมื่อผ่านการเผาซินเตอร์ที่อุณหภูมิ 900 °ซ นาน 2 ชั่วโมง

## 5. สรุปและวิจารณ์ผลการทดลอง

จากการทดลองประดิษฐ์และหาลักษณะเฉพาะของมัลติเฟร์โรอิกนาโนคอมโพสิตในระบบ บิสมัทเฟอร์ไรท์-เลดแมกนีเซียมในโอเบต-เลดไทเทเนต ที่เตรียมได้ในงานวิจัยนี้ สามารถสรุปผลการ ทดลองได้ดังนี้

- 1) สามารถเตรียมเซรามิกมัลติเฟร์โรอิกนาโนคอมโพสิตในระบบ (1-x)BF-xPT, (1-x)BF-xPMN, (1-x)BF-x(0.9PMN-0.1PT) และ (1-x)BF-x(0.7PMN-0.3PT) ที่มีสัดส่วนของ องค์ประกอบต่างๆ กันได้จากการใช้ผงที่เตรียมได้ด้วยวิธีผสมออกไซด์ ซึ่งเซรามิกมัลติ เฟร์โรอิกนาโนคอมโพสิตที่ได้จะมีเฟส โครงสร้างผลึก และโครงสร้างจุลภาคที่ เปลี่ยนแปลงไปตามสัดส่วนองค์ประกอบระหว่างเฟส BF, PMN และ PT
- 2) เซรามิกมัลติเฟร์โรอิกนาโนคอมโพสิตในระบบ (1-x)BF-xPT มีการเปลี่ยนแปลง โครงสร้างผลึกแบบรอมโบฮีดรัลไปเป็นเททระโกนอล สำหรับระบบ (1-x)BF-xPMN มี การเปลี่ยนแปลงโครงสร้างผลึกแบบรอมโบฮีดรัลไปเป็นลูกบาศก์ ในขณะที่ (1-x)BF-x(0.9PMN-0.1PT) และ (1-x)BF-x(0.7PMN-0.3PT) มีการเปลี่ยนแปลงโครงสร้างผลึก แบบรอมโบฮีดรัลไปเป็นลูกบาศก์ผสมเททระโกนอล
- 3) เซรามิกมัลติเฟร์โรอิกนาโนคอมโพสิตในระบบ (1-x)BF-xPT มีพฤติกรรมทางแม่เหล็ก เป็นแบบ superparamagnetic ในขณะที่เซรามิกมัลติเฟร์โรอิกนาโนคอมโพสิตในระบบ

- (1-x)BF-xPMN, (1-x)BF-x(0.9PMN-0.1PT) และ (1-x)BF-x(0.7PMN-0.3PT) จะแสดง พฤติกรรมทางแม่เหล็กแบบ ferromagnetic
- 4) เซรามิกมัลติเฟร์โรอิกนาโนคอมโพสิตในระบบ (1-x)BF-xPMN มีการเปลี่ยนแปลงของ ค่าคงที่ไดอิเล็กทริกตามความถี่ และมีค่าสูงสุดใน 2 ช่วงอุณหภูมิ คือที่ 230 และ 330 °ซ ซึ่งตรงกันการวิจัยที่ได้รายงานมาก่อนแล้ว

## 6. ข้อเสนอแนะ

- 1) ควรมีการควบคุมขั้นตอนการเตรียมสาร BF ให้ละเอียดมากขึ้น โดยการควบคุม บรรยากาศการเผา เพื่อให้ได้สาร BF ที่มีความบริสุทธิ์สูง
- 2) ควรทดลองศึกษาการเตรียมเซรามิกมัลติเฟร์โรอิกนาโนคอมโพสิตในระบบอื่นๆ โดยมี BF เป็นส่วนผสมหลัก และมีการควบคุมขั้นตอนในระหว่างการเตรียมและเงื่อนไขที่ใช้ใน การเผาซินเตอร์ให้มีประสิทธิภาพมากยิ่งขึ้น เช่น ใช้อุณหภูมิการซินเตอร์ที่แตกต่างกัน รวมทั้งรูปแบบการเผาซินเตอร์

## 7. เอกสารอ้างอิง

- [1] W. Eerenstein, N.D. Mathur and J.F. Scott, Nature, 442, 759 (2006).
- [2] I. Szafraniak, M. Polomska, B. Hilczer, A. Pietraszko and L. Kepinski, *J. Eur. Ceram. Soc.*, **27**, 4399 (2007).
- [3] V.A. Khomchenko, D.A. Kiselev, M. Kopcewicz, M. Maglione, V.V. Shvartsman, P. Borisov, W. Kleemann, A.M.L. Lopes, Y.G. Pogorelov, J.P. Araujo, R.M. Rubinger, N.A. Sobolev, J.M. Vieira and A.L. Kholkin, *J. Mag. Mag. Mater.*, 321, 1692 (2009).
- [4] G.A. Smolensky, V.A. Isupov and A.I. Agronovskaya, *Sov. Phys. Solid State*, **1**, 150 (1959).
- [5] C. Michel, J. M. Moreau, G. D. Achenbach, R. Gerson and W.J. James, Solid State Commun., 7, 701 (1969).
- [6] G.A. Smolenskii, V.A. Isupov, A.I. Agranovskaya and N.N. Krainik, Sov. Phys. Solid State, 2, 2651 (1961).
- [7] G.A. Smolenskii, V.M. Yudin, E.S. Sher and Y.E. Stolypin, Sov. Phys. JETP., 16, 622 (1963).
- [8] J.M. Moreau, C. Michel, R. Gerson and W.J. James, J. Phys. Chem. Solids, 32, 1315 (1971).

- [9] J. Wang, J.B. Neaton, H. Zheng, V. Nagarajan, S. B. Ogale, B. Liu, D. Viehland, V. Vaithyanathan, D. G. Schlom, U. V. Waghmare, N. A. Spaldin, K. M. Rabe, M. Wuttig and R. Ramesh, *Science*, 299, 1719 (2003).
- [10] W. Eerenstein, F.D. Morrison, J. Dho, M.G. Blamire, J.E. Scott and N.D. Mathur, *Science*, **307**, 1203a (2005).
- [11] H. Béa, M. Bibes, A. Barthélémy, K. Bouzehouane, E. Jacquet, A. Khodan, J.-P. Contour, S. Fusil, F. Wyczisk, A. Forge, D. Lebeugle, D. Colson and M. Viret, Appl. Phys. Lett., 87, 072508 (2005).
- [12] T.T. Carvalho and P.B. Tavares, Mater. Lett., 62, 3984 (2008).
- [13] J.K. Kim, S.S. Kim and W.-J. Kim, *Mater. Lett.*, **59**, 4006 (2005).
- [14] F. Chen, Q.F. Zhang, J.H. Li, Y.J. Qi, C.J. Lu, X.B. Chen, X.M. Ren and Y. Zhao, Appl. Phys. Lett., 89, 092910 (2006)
- [15] V. Fruth, L. Mitoseriu, D. Berger, A. lanculescu, C. Matei, S. Preda and M. Zaharescu, *Prog. Solid State Chem.*, **35**, 193 (2007).
- [16] S.M. Selbach, M.A. Einarsrud, T. Tybell and T. Grande, J. Am. Ceram. Soc., 90, 3430 (2007).
- [17] R. Zuo, Y. Wu, J. Fu, S. Su and L. Li, *Mater. Chem. Phys.*, **113**, 361 (2009).
- [18] M.A. Khan, T.P. Comyn and A.J. Bell, *Acta Materialia*, **56**, 2110 (2008).
- [19] G. Harshe, J.P. Dougherty ang R.E. Newnham, *Int. J. ppl. Electromagn. Mater.*, **4**, 161 (1993).
- [20] Z.Y. Li, J.G. Wang, X.W. Wang, Y. Wang, J.S. Zhu, G.H. Wang and J.-M. Liu, Integr. Ferroelectr., 87, 33 (2003).
- [21] D.R. Patil and B.K. Chougule, J. Alloys Compd., 458, 335 (2008).
- [22] J.-C. Chen and J.-M. Wua, Appl. Phys. Lett., 91, 182903 (2007).
- [23] M.T. Buscaglia, L. Mitoseriu, V. Buscaglia, I. Pallecchi, M. Viviani, P. Nanni and A.S. Siri, *J. Eur. Ceram. Soc.*, **26**, 3027 (2006).
- [24] A. Ianculescu, L. Mitoseriu, H. Chiriac, M.M. Carnasciali, A. Braileanu and R. Trusca *J. Optoel. Adv. Mater.*, **10**, 1805 (2008).
- [25] M.M. Kumar, A. Srinivas and S.V. Suryanarayana, J. Appl. Phys., 87, 855 (2000).
- [26] K. Singh, N.S. Negi, R.K. Kotnala and M. Singh, *Solid State Comm.*, **148**, 18 (2008).
- [27] T.P. Comyn, S.P. McBride and A.J. Bell, *Mater. Lett.*, **58**, 3844 (2008).
- [28] J.R. Cheng, R. Eitel and L.E. Cross, J. Am. Ceram. Soc, 86, 2111 (2003).

- [29] J.R. Cheng, N. Li and L.E. Cross, J. Appl. Phys., 94, 5153 (2003).
- [30] L. Zhang, Z. Xu, L. Cao and X. Yao, *Mater. Lett.*, **61**, 1130 (2007).
- [31] M.A. Khan, T.P. Comyn and A.J. Bell, *J. Am. Ceram. Soc.*, **88**, 2608 (2005).
- [32] R. Chen, S.-W. Yu, G.-J. Zhang, J.-R. Cheng and Z.-Y. Meng, *Trans. Nonferrous Met. Soc. China*, **16**, s116, (2006).
- [33] H. Liu and X. Wang, Solid State Comm., 147, 433 (2008).
- [34] Y. Zhou, J. Zhang, L. Li, Y. Su, J. Cheng and S. Cao, J. Alloys Compd., 484, 535 (2009).
- [35] L. Zhu, Y. Dong, X. Zhang, Y. Yao, W. Weng, G. Han, N. Ma and P. Du, *J. Alloys Compd.*, **503**, 426 (2010).
- [36] V.C. Flores, D.B. Baqués and R.F. Ziolo, Acta Materialia, 58, 764 (2010).

# Output จากโครงการวิจัยที่ได้รับทุนจาก สกว.

# 1. ผลงานวิจัยที่ตีพิมพ์ในวารสารวิชาการระดับนานาชาติ

- 1.1 M. Unruan, R. Wongmaneerung, T. Monnor, O. Khamman, W. Vittayakorn, S. Ananta and R. Yimnirun, "Dielectric Properties of Complex Perovskite PZBT-PMNT Ceramic Under Compressive Stress," Modern Physics Letter B, 25 (20011) 2391-2398.
- 1.2 R. Wongmaneerung, A. Ngamjarurojana, R. Yimnirun and S. Ananta, "Thermal Expansion and Polarization Behavior in Lead Titanate/Zinc Oxide Nanocomposite Ceramics," Key Engineering Materials, 547 (2013) 107-113.
- 1.3 R. Wongmaneerung, P. Jantaratana, R. Yimnirun and S. Ananta, "Phase Formation and Magnetic Properties of Bismuth Ferrite-Lead Titanate Multiferroic Composites," Journal of Superconductivity and Nevel Magnetism, 26 (2013) 371-379.

## 2. กิจกรรมอื่น ๆที่เกี่ยวข้อง

## การไปนำเสนอผลงานวิชาการ

- R. Wongmaneerung, R. Yimnirun and S. Ananta, "Studies on Bismuth Ferrite-Lead Titanate Multiferroic Composites," ในงานประชุมวิชาการนานาชาติ International Conference on Traditional and Advanced Ceramics (ICTA 2012). The Emerald Hotel, กรุงเทพมหานคร, ประเทศไทย
- R. Wongmaneerung, P. Jantaratana, R. Yimnirun and S. Ananta, "Magnetic Properties of (1-x)BF-xPMN Multiferroic Composites," ในการประชุมวิชาการนานาชาติ The 8<sup>th</sup> Asian Meeting Ferroelectrics (AMF 38), Amari Orchid, พัทยา, ประเทศไทย
- 3. T. Kannasut and R. Wongmaneerung, "Effect of Milling Time on Phase Formation and Physical Properties of PbFe1/2Ta1/2O3," ในการประชุมจุลทรรศน์แห่งประเทศไทย ครั้งที่ 30 (MST30), รีสอร์ทมณีจันท์, จันทบุรี, ประเทศไทย

## รางวัลที่ได้รับ

- 1. รางวัลงานวิจัยของคณะวิทยาศาสตร์ ด้านผลงานวิจัยที่มีผู้อ้างอิงมากที่สุดของบุคลากรคณะ วิทยาศาสตร์ มหาวิทยาลัยแม่โจ้ ประจำปี 2554
- 2. รางวัลงานวิจัย ด้านนักวิจัยที่มีผลงานวิจัยที่ได้รับการอ้างอิงมากที่สุด สาขาวิทยาศาสตร์และ เทคโนโลยี มหาวิทยาลัยแม่โจ้ ประจำปี 2555

#### ภาคผนวก

- 1. รายงานการวิจัยที่ได้จัดส่งลงตีพิมพ์ในวารสารทางวิชาการระดับนานาชาติ
- 2. Manuscript ที่ได้จัดส่งวารสาร Materials Chemistry and Physics
- 3. Manuscript ที่ได้จัดส่งวารสาร Journal of Superconductivity and Novel Magmetism
- 4. การเสนอผลงานทางวิชาการระดับชาติและนานาชาติ
- 5. รางวัลที่ได้รับ

## รายงานการวิจัยที่ได้จัดส่งลงตีพิมพ์ในวารสารทางวิชาการระดับนานาชาติ

Modern Physics Letters B, Vol. 25, No. 31 (2011) 2391–2398  $\odot$  World Scientific Publishing Company DOI: 10.1142/S0217984911027716



# DIELECTRIC PROPERTIES OF COMPLEX PEROVSKITE PZBT-PMNT CERAMIC UNDER COMPRESSIVE STRESS

#### MUANGJAI UNRUAN\*, TEERAWAT MONNOR and RATTIKORN YIMNIRUN†

School of Physics, Institute of Science, Suranaree University of Technology, Nakhon Ratchasima 30000, Thailand  $^*muangjaiunruan@yahoo.com \\ ^\dagger rattikorn@sut.ac.th$ 

#### ORAWAN KHAMMAN<sup>‡</sup>, WANWILAI VITTAYAKORN<sup>§</sup> and SUPON ANANTA¶

Department of Physics, Faculty of Science, Chiang Mai University,

Chiang Mai, 50200, Thailand

† orawan2006@yahoo.com

§ sum\_oil@hotmail.com

¶ supon@chiangmai.ac.th

#### REWADEE WONGMANEERUNG

Program in Materials Science, Faculty of Science, Mae Jo University, Chiang Mai, 50290, Thailand rewadeewongmaneerung@hotmail.com

Received 19 December 2008

Effects of compressive stress on the dielectric properties of complex perovskite PZBT-PMNT ceramic were investigated. The dielectric properties measured under stress-free condition showed a composite nature with two distinct temperatures of dielectric maximum associated with PZBT and PMNT end members. The dielectric properties under the compressive stress were observed at stress levels up to 230 MPa using a home-built compressometer. The results clearly showed that the compression load significantly reduced both the dielectric constant and the dielectric loss tangent in every measuring frequency. The change of the dielectric constant with stress was attributed to competing influences of the intrinsic contribution of non-polar matrix and the extrinsic contributions of re-polarization and growth of micro-polar regions, while the clamping of the domain walls contributed to the stress-dependent changes of the dielectric loss tangent. Finally, a large drop of the dielectric constant after a stress cycle was likely caused by the stress induced decrease in switchable part of spontaneous polarization.

Keywords: Dielectric properties; PZBT-PMNT; compressive stress.

#### 1. Introduction

Complex perovskite ferroelectric ceramics have been studied extensively with potential applications in several micro- and nano-electronic devices such as multilayer capacitors, micro-actuators and miniaturized transducers. $^{1-5}$  Barium

titanate (BaTiO<sub>3</sub> or BT), lead titanate (PbTiO<sub>3</sub> or PT), lead zirconate titanate (Pb(Zr<sub>1-x</sub>Ti<sub>x</sub>)O<sub>3</sub> or PZT), lead magnesium niobate (Pb(Mg<sub>1/3</sub>Nb<sub>2/3</sub>)O<sub>3</sub> or PMN) ceramics and a variety of their solid solutions have been investigated extensively and continuously since the late 1940s. <sup>1,3,4</sup> Two of the most studied ferroelectric compounds, PZT and BT ceramics are representative perovskite piezoelectric and ferroelectric prototypes, respectively. While BT has a high dielectric constant with a relatively low Curie temperature ( $T_C$ ) (~120°C), PZT has a higher  $T_C$  of 390°C which allows PZT-based piezoelectric devices to be operated at relatively higher temperatures. <sup>2,4</sup> Although BT ceramic has better mechanical properties than PZT, the sintering temperature is also higher. <sup>1,3,6</sup> Thus, a mixture of PZT and BT is expected to decrease the sintering temperature of BT-based ceramics while maintaining excellent electrical properties of the end members. Our previous investigations have already shown the optimized electrical properties in 0.5PZT-0.5BT ceramic with  $\varepsilon_T \sim 4000$  at  $T_C$  of 160°C. <sup>7,8</sup>

Lead-based relaxor ferroelectrics are the other family of ferroelectric materials which are of great interest due to their high polarizabilities. One of the most widely studied in this family is PMN, which has very good dielectric properties.  $^{2,3,5}$  However, PMN has very low temperature related to the maximum dielectric constant  $(T_{\rm max})$  ( $\sim -10^{\circ}{\rm C}$ ). Therefore, PT is usually added to PMN to enhance the dielectric properties of PMN (as well as increasing  $T_{\rm max}$ ). In particular, 0.9PMN-0.1PT ceramics, which have  $T_{\rm max} \sim 40^{\circ}{\rm C}$  and  $\varepsilon_{r,{\rm max}} > 20000$ , have been widely applied for capacitor, actuator and transducer applications. However, since there have always been a need to obtain ceramic with broad dielectric peak and maximum dielectric constant for various applications, especially in capacitive components,  $^{2-5}$  and with the complimentary characteristics between 0.5PZT-0.5BT and 0.9PMN-0.1PT ceramics, it is expected that excellent dielectric properties can be obtained from a mixture composition of the two ceramic systems. It is, therefore, one of the aims of this study to explore the dielectric properties of the mixture composition of 0.5PZT-0.5BT and 0.9PMN-0.1PT.

However, it is well known that the electrical properties of ferroelectric materials depend significantly on mechanical stress.<sup>13-15</sup> Many previous investigations reported the significant changes in electrical properties of ferroelectric materials under compressive stress.<sup>15-22</sup> Therefore, the major aim of this study is to investigate the influences of the compressive stress on the dielectric properties of complex perovskite PZBT-PMNT ceramic.

#### 2. Experimental Details

The ceramic composition with a formula  $[0.5Pb(Zr_{0.52}Ti_{0.48})O_3-0.5BaTiO_3]-[0.9Pb(Mg_{1/3}Nb_{2/3})O_3-0.1PbTiO_3]$  (abbreviated as PZBT-PMNT hereafter) was chosen for this study. The PZBT-PMNT powders were prepared from  $0.5Pb(Zr_{0.52}Ti_{0.48})O_3-0.5BaTiO_3$  (abbreviated as PZBT hereafter) and  $0.9Pb(Mg_{1/3}-Nb_{2/3})O_3-0.1PbTiO_3$  (abbreviated as PMNT hereafter) starting

powders via a simple mixed-oxide method.<sup>7,23</sup> The detailed descriptions of the PZBT and PMNT powders processing and characterization were presented in previous reports and will not be discussed here. 7,8,23 The PZBT-PMNT ceramics were then fabricated via the same mixed-oxide method. After mixing the powders by ball-milling method and drying process, the mixed powders were pressed hydraulically to form disc-shaped pellets 10 mm in diameter and 2 mm thick, with 3 wt.% polyvinyl alcohol as a binder. The PZBT-PMNT green pellets were placed on the alumina powder-bed inside alumina crucible and surrounded with atmosphere powders of the same composition. Finally, the pellets were sintered in air at 1250°C for 2 h.

For dielectric characterizations, the sintered specimens were carefully lapped to obtain parallel faces disc-shaped specimens with diameter of 8 mm and thickness of 1 mm, and the faces were then coated with silver paint as electrodes. The samples were subsequently heat-treated at 750°C for 12 min to ensure the contact between the electrodes and the ceramic surfaces. The dielectric properties of the sintered ceramics were examined under stress-free condition as functions of both temperature and frequency with an automated dielectric measurement system over the temperature range of 25°C and 300°C with the frequency ranging from 1 kHz to 1 MHz. To study the effects of the compressive stress on the dielectric properties, the uniaxial compressometer was constructed. 20,24 The dielectric properties were measured by LCR-meter (Instrek LCR-821). The room temperature (25°C) capacitance and the dielectric loss tangent were obtained at frequency range 10 kHz to 200 kHz under the compressive stress levels up to 230 MPa.

#### 3. Results and Discussion

The temperature and frequency-dependent dielectric properties, e.g. dielectric constant  $(\varepsilon_r)$  and dielectric loss  $(\tan \delta)$ , are plotted in Fig. 1. Two distinct dielectric anomalies are clearly observed. The first dielectric peak at lower temperature region with higher dielectric constant is associated with the PMNT component, which has  $T_{\rm max}$  near 40°C.<sup>2</sup> A strong dielectric dispersion below  $T_{\rm max}$  also indicates a relaxor ferroelectric behavior. The temperatures of maximum dielectric constant and dielectric loss tangent are also seen shifted to higher temperature with increasing frequency. The maximum value of the dielectric constant decreases with increasing frequency, while that of the dielectric loss tangent increases. The dielectric properties then become frequency independence above the transition temperature. 25,26 Even though these descriptions are not clearly seen on the first dielectric peak because of the close appearance of the second dielectric peak, it could still be said that the relaxor behavior exists in the ceramic system. The second dielectric peak occurs over temperature range 150-200°C, which should be associated with the PZBT component with  $T_C$  near  $162^{\circ}$ C.<sup>7,8</sup> A diffuse phase transition with small frequency dispersion of the dielectric maxima is also observed within this second dielectric peak, similar to earlier reported observation for the

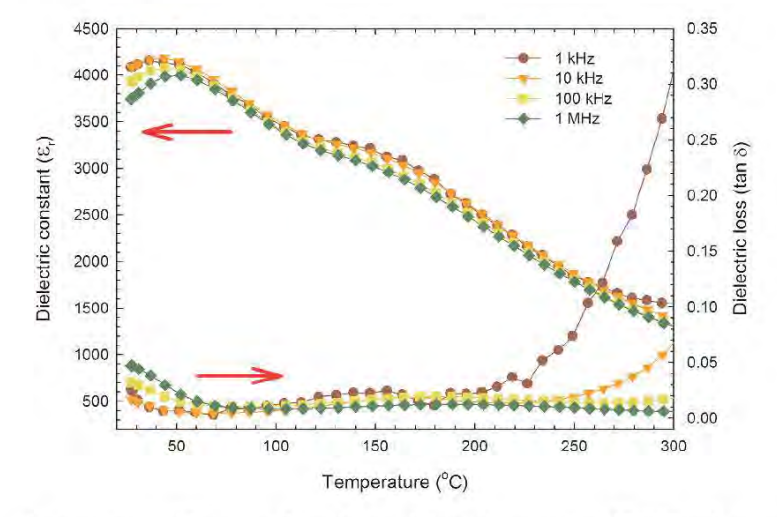


Fig. 1. Temperature and frequency dependences of dielectric properties of PZBT under stress-free condition.

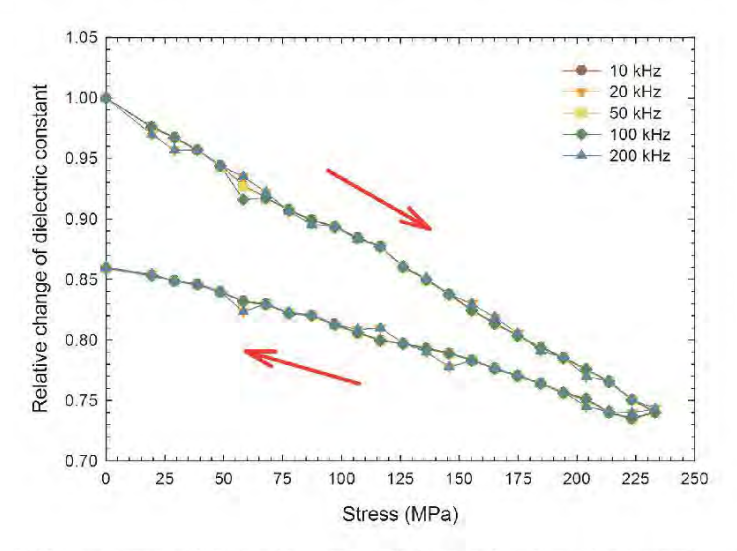


Fig. 2. Relative changes of dielectric constant  $(\varepsilon_r)$  as a function of compressive stress for PZBT-PMNT ceramic (solid arrows indicate loading direction).

PZBT component.<sup>8</sup> These observations of the two distinct dielectric peaks should indicate the composite nature of the PZBT-PMNT ceramic. A significant increase in the dielectric constant and dielectric loss at high temperatures is attributed to the thermally activated space charge conduction.<sup>25,26</sup>



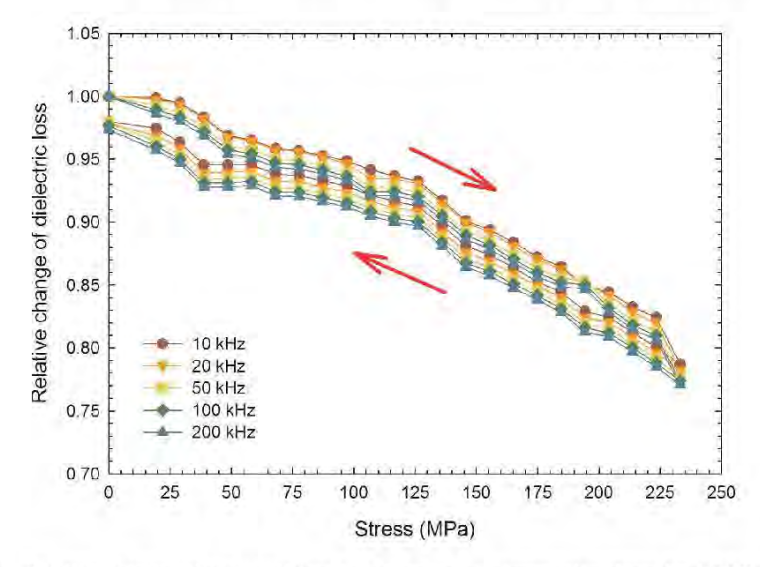


Fig. 3. Relative changes of dielectric loss as a function of compressive stress for PZBT-PMNT ceramic (solid arrows indicate loading direction).

The fractional changes of the dielectric properties of the PZBT-PMNT ceramic under the compressive stress during loading and unloading are shown in Figs. 2 and 3. With increasing stress from 0 to 230 MPa and returning to stress-free condition, a significant change of the dielectric properties of the ceramic system is clearly observed. The dielectric constant decreases with increasing stress, then increases only slightly when the compressive stress is gradually removed, as displayed in Fig. 2. However, it should be noticed that the changing of the dielectric constant with loading and unloading stress does not follow the same path. In every frequency, the dielectric constant with increasing the compressive stress is larger in value than that with decreasing stress. Interestingly, the stress-free dielectric constant value is also decreased significantly after a stress cycle. The dielectric constant is seen to decrease as much as 25% at the maximum stress and only returns to about 85% of its original value when the stress is removed. Interestingly, Fig. 3 shows that the change in the dielectric loss tangent value is less significant, as it only decreases about 10-20% at the maximum stress and almost returns to its original value after a stress cycle. Previous investigations in other ceramic systems, such as BT, PZT, PMN, PMN-PT and PMN-PZT, have also reported similar observations. 17,20,22,27,28

Various effects, i.e. the intrinsic contribution of domains and extrinsic contributions of re-polarization and growth of micro-polar regions have to be considered to explain the changes when ferroelectric materials subjected to compressive stress. 16,17,20,22,27,28 The situation for the PZBT-PMNT system is quite complex because this system is a mixing between the relaxor ferroelectric PMNT and the normal ferroelectric PZBT. There is thus a competing mechanism between the two different types of materials. In this study, as the dielectric properties was measured under the application of stress at room temperature  $(\sim 25^{\circ}\text{C})$  (below the  $T_{\text{max}}$  of PMNT  $(\sim 40^{\circ}\text{C})$ ), <sup>12</sup> the stress-dependent dielectric properties of the PZBT-PMNT ceramic should be dominated by the contribution from relaxor ferroelectric PMNT. Therefore, the decreases in both dielectric constant and dielectric loss tangent with increasing stress can be attributed to competing influences of the intrinsic contribution of non-polar matrix and the extrinsic contribution of re-polarization and growth of micro-polar regions, which respond to the applied stress in an opposite way. As mentioned above, the non-polar matrix contribution from relaxor ferroelectric PMNT is expected to dominate in this case. 27,28 Hence, the dielectric responses to the compressive stress in the PZBT-PMNT ceramic are observed to decrease significantly with increasing stress, as observed in Figs. 2 and 3. In addition, a significant decrease in the dielectric constant after a full cycle of stress application has been observed, and attributed to the stress induced decrease in switchable part of spontaneous polarization at high stress. 21,29 The stress clamping of domain walls is believed to be the cause of the decrease in dielectric loss. 22,27 This phenomenon reduces the domain mobility that causes the reduction of dielectric loss. This is a reversible effect which results in the dielectric loss returning to near original values after the applied stress is removed, as seen in Fig. 3.

Finally, it is worth-noting that our earlier investigations on the stress-dependent dielectric properties of the two members, i.e. PZBT<sup>30</sup> and PMNT,<sup>22</sup> revealed that under a similar stress condition the dielectric constant of the PMNT ceramic decreased nearly 70%, whereas the PZBT ceramic showed approximately 5–10% increase in the dielectric constant, at maximum stress level. Clearly, the apparent suppression of changes in the dielectric constant with stress observed in this present study supports the composite nature of the PZBT-PMNT ceramic, as also revealed by the free-stress dielectric properties measurements shown in Fig. 1.

#### 4. Conclusion

The stress-dependent dielectric properties of complex perovskite PZBT-PMNT ceramic were investigated in this study. The dielectric properties measured under stress-free condition showed two distinct dielectric peaks associated with PZBT and PMNT. The homebuilt compressometer was employed to examine the dielectric properties under the influence of the compressive stress. It was found that the superimposed compression load significantly reduced both the dielectric constant and the dielectric loss tangent in every measuring frequency. The change of the dielectric properties with stress was attributed mainly to the dominant contribution from the non-polar matrix of the relaxor ferroelectric PMNT end member. Other contributions include the clamping of the domain walls and the stress induced decrease in switchable part of spontaneous polarization. This study

clearly indicated that the complex perovskite PZBT-PMNT ceramic possessed a composite nature.

#### Acknowledgments

MU and RY acknowledge the financial support from the Higher Education Research Promotion and National Research University Project of Thailand, Office of the Higher Education Commission and Suranaree University of Technology.

#### References

- 1. B. Jaffe and W. R. Cook, Piezoelectric Ceramics (R.A.N. Inc., New York, 1971).
- 2. L. E. Cross, Mater. Chem. Phys. 43 (1996) 108.
- 3. G. H. Haertling, J. Am. Ceram. Soc. 82(4) (1999) 797.
- 4. N. Setter, J. Euro. Ceram. Soc. 21 (2001) 1279.
- A. J. Moulson and J. M. Herbert, Electroceramics: Materials, Properties, Applications, 2nd edn. (John Wiley & Sons, New York, 2003).
- 6. W. Chaisan, S. Ananta and T. Tunkasiri, Curr. Appl. Phys. 4 (2004) 182.
- 7. W. Chaisan, R. Yimnirun, S. Ananta and D. P. Cann, Mater. Lett. 59 (2005) 3732.
- W. Chaisan, R. Yimnirun, S. Ananta and D. P. Cann, Mater. Sci. Eng. B 132 (2006) 300.
- 9. S. Jiang, D. Zhou, S. Gong and W. Lu, Sensors Actuat. A 69 (1998) 1.
- 10. Y. C. Liou, J. Mater. Sci. 103 (2003) 281.
- 11. A. Safari, R. K. Panda and V. F. Janas, Appl. Ferro. Ceram. Mater. 1 (2000) 1.
- 12. S. Huang, C. Feng, L. Chen and X. Wen, Integr. Ferroelectr. 74 (2005) 45.
- 13. L. E. Cross, Ferroelectrics **76** (1987) 241.
- Y. H. Xu, Ferroelectric Materials and Their Applications (North Holland, Los Angeles, 1991).
- 15. D. Viehland and J. Powers, J. Appl. Phys. 89(3) (2001) 1820.
- 16. J. Zhao, A. E. Glazounov and Q. M. Zhang, Appl. Phys. Lett. 74 (1999) 436.
- 17. Q. M. Zhang, J. Zhao, K. Uchino and J. Zheng, J. Mater. Res. 12 (1997) 226.
- D. Viehland, J. F. Li, E. McLaughlin, J. Powers, R. Janus and H. Robinson, J. Appl. Phys. 95 (2004) 1969.
- 19. D. Zhou, M. Kamlah and D. Munz, J. Euro. Ceram. Soc. 25 (2005) 425.
- R. Yimnirun, S. Ananta, E. Meechoowas and S. Wongsaenmai, J. Phys. D: Appl. Phys. 36 (2003) 1615.
- R. Yimnirun, S. Wongsaenmai, A. Ngamjarurojana and S. Ananta, Curr. Appl. Phys. 6 (2006) 520.
- R. Yimnirun, M. Unruan, Y. Loasiritaworn and S. Ananta, J. Phys. D: Appl. Phys. 39 (2006) 3097.
- R. Wongmaneerung, T. Sarakonsri, R. Yimnirun and S. Ananta, Mater. Sci. Eng. B 132 (2006) 292.
- R. Yimnirun, S. Ananta, A. Ngnamjarurojana and S. Wongsaenmai, Appl. Phys. A: Mater. 81(6) (2005) 1227.
- 25. R. Yimnirun, S. Ananta and P. Laoratanakul, Mater. Sci. Eng. B 112 (2004) 79.
- R. Yimnirun, S. Ananta and P. Laoratanakul, J. Euro. Ceram. Soc. 25(13) (2005) 3225.
- G. Yang, W. Ren, S. F. Liu, A. J. Masys and B. K. Mukherjee, Proc. IEEE Ultra Symp. 1 (2000) 1005.

2398 M. Unruan et al.

- 28. O. Steiner, A. K. Tagantsev, E. L. Colla and N. Setter, J. Euro. Ceram. Soc. 19 (1999) 1243.
  29. J. Zhao and Q. M. Zhang, Proc. IEEE ISAF 2 (1996) 971.
  30. R. Yimnirun, Ferroelectrics 331 (2006) 9.

## Thermal Expansion and Polarization Behavior in Lead Titanate/Zinc Oxide Nanocomposite Ceramics

R. Wongmaneerung<sup>1,a</sup>, A. Ngamjarurojana<sup>2,b</sup>, R. Yimnirun<sup>3,c</sup> and S. Ananta<sup>2,d</sup>
<sup>1</sup>Department of Materials Science, Maejo University, Chiang Mai, 50290, Thailand
<sup>2</sup>Department of Physics and Materials Science, Chiang Mai University, Chiang Mai, 50200, Thailand

<sup>3</sup>School of Physics, Institute of Science, Suranaree University of Technology, Nakhon Ratchasima 30000, Thailand

<sup>®</sup>re\_nok@yahoo.com, <sup>b</sup>ngamjarurojana@yahoo.com, <sup>c</sup>rattikornyimnirun@yahoo.com, <sup>d</sup>suponananta@yahoo.com

Keywords: Polarization behavior, Thermal expansion, Lead titanate, Nanocomposite

Abstract. This study examined nanosized zinc oxide/lead titanate (ZnO/PT) ceramic matrix nanocomposites. Under an appropriate sintering condition, ZnO/PT ceramic nanocomposites were successfully fabricated using a pressureless sintering technique. Thermal expansion and polarization behaviors were determined by using a dilatometer. This technique measures the temperature-dependence of the strain, and the magnitude of polarization can be deduced from the sets of thermal expansion data. The calculated electric polarization values on the ZnO/PT nanocomposite ceramics demonstrated a simple approach to determine the temperature dependence of the polarization below and around the transition temperature. Various aspects of understanding the polarization behavior and other effects in the ferroelectric are discussed.

#### Introduction

It is well known that material properties depend on processing methods governed by the processing parameters, through their thermal and electrical properties. Today, nanotechnology has emerged as a novel approach to improving material properties [1,2]. To improve the dielectric properties of ferroelectric ceramics, nanocomposites consisting of two or more materials with different macroscopic properties are more attractive than their single-phase counterparts. Lead titanate (PT) ceramic based composites have recently been developed to improve the mechanical and dielectric properties [3–5]. In our previous work [4,5], silicon carbide (SiC) nanofibers and zine oxide (ZnO) nanowhiskers were employed as the reinforcement in the composites because of their ability to resist crack growth. ZnO has received much attention as a reinforcement composite material due to its high-temperature strength and excellent chemical stability [5]. Moreover, microstructural evolution and the dielectric properties of ZnO/PT ceramic nanocomposites have been reported and the results have shown complex microstructures that are inherently heterogeneous. This factor has an important effect on the dielectric properties of the materials. However, due to the heterogeneity of these materials, no work on thermal expansion and spontaneous polarization (P<sub>S</sub>) of ZnO/PT composites has been reported.

A variety of experimental techniques, including refractive index measurements [6], Raman scattering [7], neutron powder diffraction [8], neutron elastic scattering [9] and dynamic light scattering [10] has been employed to confirm the value of  $P_{\rm S}$ . The change in polarization with temperature can be observed through thermal expansion (or strain) measurements and from the data,  $P_{\rm S}$  can be computed. It is always a challenge to measure the temperature-dependence of the polarization of the high Curie temperature ( $T_{\rm C}$ ) ferroelectric over the entire temperature range. Therefore, alternative approaches have to be employed to extract useful data on ZnO/PT for the polarization versus temperature behavior. From the phenomenological approach we know that the  $P_{\rm S}$  values can be extracted by using the relation [11]:

All rights reserved. No part of contents of this paper may be reproduced or transmitted in any form or by any means without the written permission of TTP, www.ltp.net. (ID: 202.28.38.171-14/02/13,05:13/44)

$$x_{ij} = \frac{\Delta I}{I} = Q_{ijkl}P_k^2$$
(1)

where  $x_{ij}$  is the strain,  $\Delta l/l$  is thermal expansion and  $Q_{ijkk}$  is the electrostrictive coefficient. Q coefficients are determined in the paraelectric phase and considered constant. In addition,  $P_k^2$  is the polarization. Also, by knowing the  $\Delta l/l$  and its temperature dependence,  $P_k$  versus temperature as well as the transition temperature of ZnO/PT and the nature of the transition can be studied.

In this paper, we report the  $P_{\rm S}$  versus temperature behavior of ZnO/PT ceramic nanocomposites. We have measured the thermal expansion versus temperature behavior and computed the values of polarization at various temperatures. We also obtained the polarization values from the ferroelectric hysteresis (P-E) measurements.

#### Experimental

The starting pure PT powders were synthesized using a simple mixed oxide method. The average particle size of powders is about 1.5 µm. Two different shapes of reinforced ZnO nanoparticles: nanopowders (P) and nanotripods (T) with pure PT matrix, were investigated. The ZnO/PT nanocomposite ceramics were prepared using the conventional solid-state reaction and pressurcless sintering technique. The different amounts (0.5 and 1 wt%) of ZnO were ultrasonically dispersed in ethanol for 30 min before mixing with the PT powders. Ceramics fabrication was achieved by adding 3 wt% polyvinyl alcohol binder prior to pressing as a pellet in a pseudo-uniaxial die press at 100 MPa. Each pellet was placed in an alumina crucible together with an atmosphere powder of identical chemical composition. Sintering was carried out with a dwell time of 2 h, with constant heating/cooling rates of 5 °C/min and sintering temperature set at 1200 °C.

For thermal expansion measurement, all samples were cut in bar shapes (3 mm long and 1 mm thick), placed inside a fused silica holder, and heated at a rate of 5 °C/min from 25 °C to 600 °C and the thermal expansion was measured as a function of temperature using a push-rod type differential dilatometer. Ferroelectric hysteresis measurements were made using a modified Sawyer-Tower circuit controlled by a computer.

#### Results and Discussion

The thermal expansion behaviors of ZnO/PT ceramic nanocomposites were measured using a high-sensitivity dilatometer. The results are shown in Figs. 1 and 2. One can see that most of these compositions exhibit negative thermal expansion. Table 1 summarizes the various important features derived from the thermal strain versus temperature measurements. Noted that the thermal expansion measurements were made during the first heating from room temperature. The results show that the thermal expansion behaviors of these samples are linear at temperatures above 500 °C, (i.e., above Curie temperature). The change of strain at the Curie point is easily seen in the thermal contraction curves. This indicates that the respective paraelectric–ferroelectric phase transition occurs at 469 °C and 468 °C for samples with 0.5 and 1 %wt with ZnO nanotripods. The phase transition temperatures from thermal strain are in good agreement with the published values from dielectric measurements [3,5]. Moreover, One can see that with increasing ZnO content, T<sub>C</sub> shifted toward lower temperatures. The shift of the phase transformation temperature in these ZnO/PT composites might be due to a relaxation of transformation-induced internal stress by the ZnO dispersed in the PT matrix [5].

TABLE 1 Summary of the various important features of the thermal expansion measurements

Sample	T <sub>C</sub> (°C)	Calculated $P_S$ at room temperature ( $\mu$ C/cm <sup>2</sup> )	
1 PbTiO <sub>3</sub>	489	75.0	
2 PT/0.5 %wt ZnO nanopowders	469	77.4	
3 PT/1.0 %wt ZnO nanopowders	468	78.1	
4 PT/0.5 %wt ZnO nanotripods	470	77.0	
5 PT/1.0 %wt ZnO nanopowders	468	76.7	

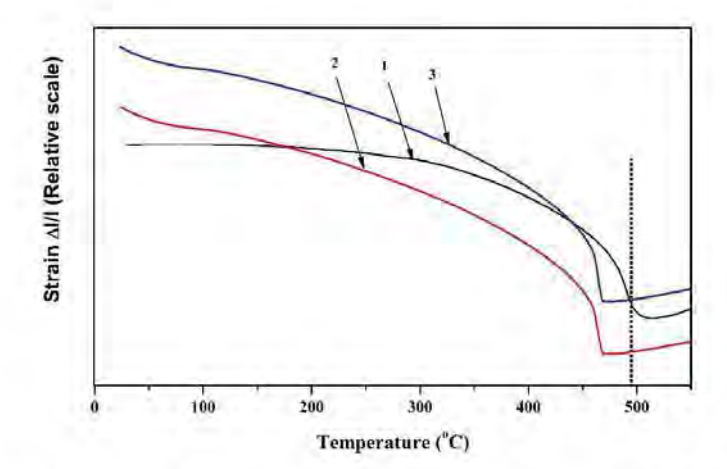


Fig. 1 Strain as a function of temperature for PT ceramic nanocomposites with different ZnO content: (1) pure PT, (2) 0.5 %wt ZnO nanopowders and (3) 1.0 %wt ZnO nanopowders (all measurements are in heating cycles).

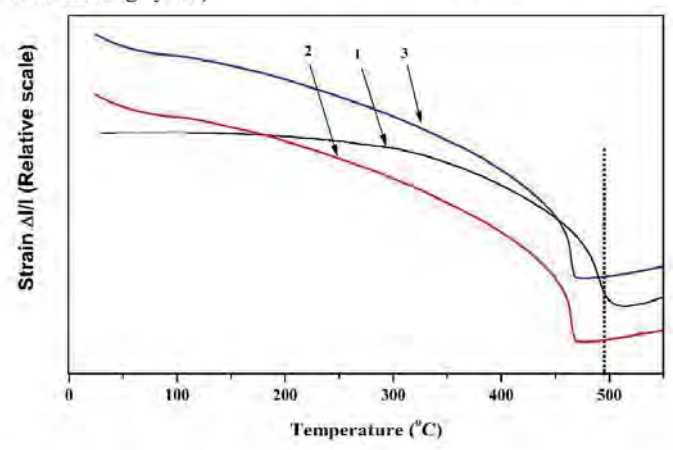


Fig. 2 Strain as a function of temperature for PT ceramic nanocomposites with different ZnO content: (1) pure PT, (2) 0.5 %wt ZnO nanotripods and (3) 1.0 %wt ZnO nanotripods (all measurements are in heating cycles).

At temperatures below Curie temperature, these linear thermal expansions are superimposed by a ceramics' spontaneous polarization. The high temperature data in the cubic phase, above  $T_C$ , can be approximated by a straight line. The deviation from this linear high temperature behavior occurs at approximately the same temperature ( $\sim 500^{-9}$ C). On analyzing the deviation of the strain from the high temperature linear behavior and by using Eq. (1) the  $P_S$  values can be obtained at various temperatures. Using the values of  $Q_{11} = 8.9 \times 10^{-2}$  m<sup>4</sup>/C<sup>2</sup> and  $Q_{12} = -2.6 \times 10^{-2}$  m<sup>4</sup>/C<sup>2</sup> [12], the  $P_S$  can be calculated. The results for various samples are plotted in Figs. 3 and 4. When calculating the spontaneous strains of the tetragonal cell at a particular temperature, the cubic cell constant should be extrapolated to that temperature accounting for the thermal expansion. A linear extrapolation from above the transition can be made over a narrow range with fairly good accuracy.

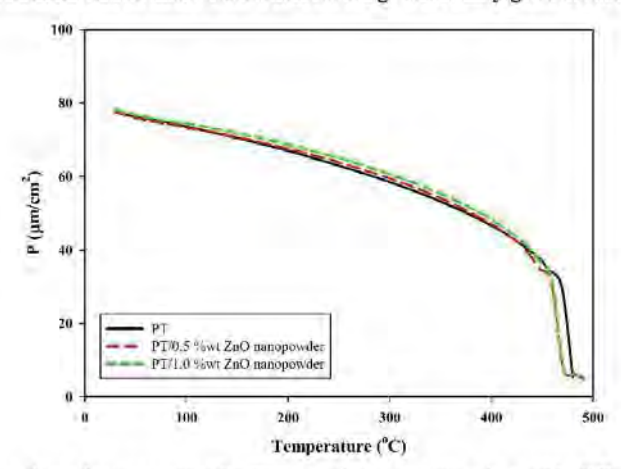


Fig. 3  $P_{\rm S}$  as a function of temperature for PT ceramic nanocomposites with different ZnO content: (1) pure PT, (2) 0.5 %wt ZnO nanopowders and (3) 1.0 %wt ZnO nanopowders.

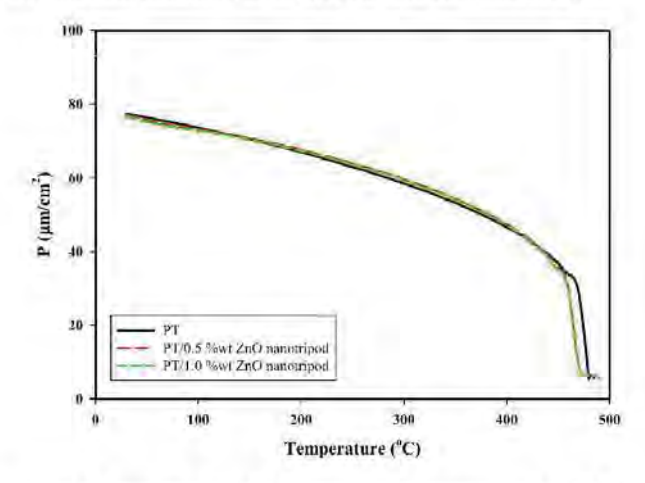


Fig. 4  $P_S$  as a function of temperature for PT ceramic nanocomposites with different ZnO content: (1) pure PT, (2) 0.5 %wt ZnO nanotripods and (3) 1.0 %wt ZnO nanotripods.

Figs. 3 and 4 show the  $P^2 = \sqrt{P_E^2}$  values calculated from the thermal expansion data. The agreement in the  $P_S$  values is excellent. The values are also in good agreement not only in magnitude but also in the  $T_C$  values with the earlier reported results [5,13]. Fig. 3 shows the  $P_S$  value versus temperature of PT ceramic with different contents of ZnO nanopowders. The  $P_S$  value in this case is slightly higher than those of pure PT samples in temperature range below the Curie point. Also, similar trends were noticed in samples with added ZnO nanotripods and sintered under the same conditions. One can see that the magnitude of  $P_S$  and trend of polarization behavior are similar to that of ZnO/PT nanopowders. Moreover, the polarization behavior for all samples shows a sharp first-order phase transition. Several factors could have influenced the measurements. These include contributions to the strain in ferroelectrics, (i.e., in addition to the structural component which is present at all temperatures, a component associated with the appearance of spontaneous polarization in the case of ferroelectric state is also present). The contribution of the spontaneous polarization to strain is due to electrostrictive coupling [13].

Also plotted in Figs. 5 and 6 are the normal reversible polarization data,  $P_r$ , determined from the P-E measurements. It is evident that the polarization calculated from the strain is larger than  $P_r$  and extends several hundred degrees above  $T_C$  due to quadratic electrostrictive effects. Moreover, for temperatures well below  $T_C$ , although not equal,  $P_S$  and  $P_r$  are comparable; they are obtained by totally independent techniques. The strain measurements can detect this effect because  $P_S^2$  rather than  $P_S$  contributes to these terms. Once local regions of polarization occur, the cooperative effect that occurs at  $T_C$  can be understood.

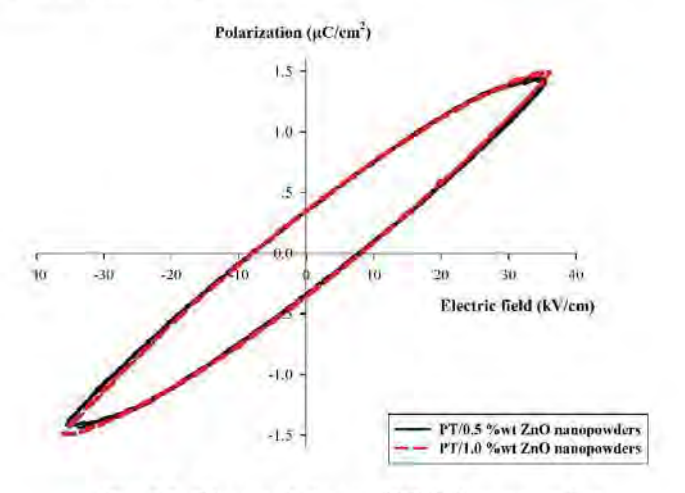


Fig. 5 P-E hysteresis loops of PT/ZnO nanopowders.

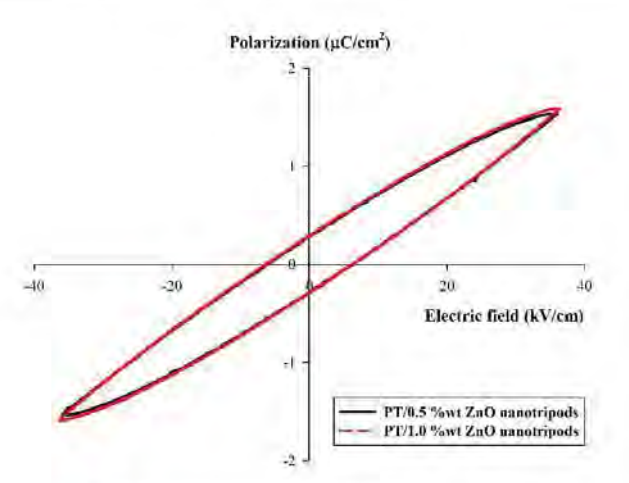


Fig. 6 P-E hysteresis loops of PT/ZnO nanotripods.

#### Conclusions

This research reports anolmaly behavior of thermal expansion in ZnO/PT ceramic nanocomposites. The room temperature  $P_{\rm S}$  in range of 76–78  $\mu$ C/cm<sup>2</sup> is in good agreement with the reported values, suggesting that thermal strain data can be used reliably for estimating polarization behavior and its temperature dependence in the case of high  $T_{\rm C}$  ferroelectrics or where the high conductivity of samples interferes with electrical measurements.

#### **Acknowledgments**

We thank the Thailand Research Fund (TRF) and the Faculties of Science of Maejo University. Also acknowledged for providing additional support during this work is Processing Technology of Materials Research Laboratory (PTMRL).

#### References

- K. Niihara, New design concept of structural ceramics; ceramic nanocomposites, J. Am. Ceram. Soc. 99 (1991) 974–982.
- [2] T. Ohji, Y.K. Jeong, Y.H. Choa, K. Niihara, Strengthening and toughening mechanisms of ceramic nanocomposites, J. Am. Ceram. Soc. 81 (1998) 1453–1460.
- [3] R. Wongmaneerung, A. Rujiwatra, R. Yimnirun, S. Ananta, Fabrication and dielectric properties of lead titanate nanocomposites, J. Alloys Compd. 475 (2009) 473–478.
- [4] R.Wongmaneerung, P. Singjai, R. Yimnirun, S. Ananta, Effects of SiC nanofibers addition on microstructure and dielectric properties of lead titanate ceramics, J. Alloys Compd. 475 (2009) 456–462.
- [5] R. Wongmaneerung, S. Choopan, R. Yimnirun, S. Ananta, Dielectric properties of PbTiO<sub>3</sub>/ZnO ceramic nanocomposites obtained by solid-state reaction method, J. Alloys Compd. 509 (2011) 3547–3552.
- [6] G. Burns, F.H. Dacol, Polarization in the cubic phase of BaTiO<sub>3</sub>, Solid State Commun. 42 (1982) 9-12.
- [7] G. Burns, F.H. Dacol, Soft phonons in a ferroelectric polarization glass system, Solid State Commun. 58 (1986) 567–571.

- [8] J. Zhao, A.E. Glazounov, Q.M. Zhang, B. Toby, Neutron diffraction study of electrostrictive coefficients of prototype cubic phase of relaxor ferroelectric PbMg<sub>1/3</sub>Nb<sub>2/3</sub>O<sub>3</sub>, Appl. Phys. Lett. 72 (1998) 1048–1050.
- [9] D. La-Orauttapong, J. Toulouse, Z.-G. Ye, W. Chen, R. Erwin, J.L. Robertson, Neutron scattering study of the relaxor ferroelectric (1-x)Pb(Zn<sub>1/3</sub>Nb<sub>2/3</sub>)O<sub>3</sub>-xPbTiO<sub>3</sub>, Phys. Rev. B 67 (2003) 134110-134120.
- [10] W. Kleemann, P. Licinio, T.Woike, R. Pankrath, Dynamic light scattering at domains and nanoclusters in a relaxor ferroelectric, Phys. Rev. Lett. 86 (2001) 6014–6017.
- [11] A.S. Bhalla, R. Guo, L.E. Cross, Measurements of strain and the optical indices in the ferroelectric Ba<sub>0.4</sub>Sr<sub>0.6</sub>Nb<sub>2</sub>O<sub>6</sub>: polarization effects, Phys. Rev. B. 36 (1987) 2030–2035.
- [12] M. J. Huan, E. Furman, S. J. Jang, H. A. McKinstry, L. E. Cross, Thermodynamic theory of PbTiO<sub>3</sub>, J. Appl. Phys. 62 (1987) 3331–3338.
- [13] R. Wongmaneerung, R. Yimnirun, S. Ananta, R. Guo, A. S. Bhalla, Polarization behavior in the two stage sintered lead titanate ceramics, Ferroelectric Lett., 33 (2006) 137–146.

#### ORIGINAL PAPER

## Phase Formation and Magnetic Properties of Bismuth Ferrite-Lead Titanate Multiferroic Composites

R. Wongmaneerung · P. Jantaratana · R. Yimnirun · S. Ananta

Received: 5 June 2012 / Accepted: 9 July 2012 / Published online: 25 July 2012 © Springer Science+Business Media, LLC 2012

Abstract In this study, phase formation and the magnetic properties of bismuth ferrite-lead titanate multiferroic composites were investigated. Multiferroic composites consisting of antiferromagnetic bismuth ferrite (BiFeO3 or BF) and ferroelectric lead titanate (PbTiO3 or PT) were synthesized by the solid-state sintering method. The presence of pure phase in these composites was confirmed by Xray diffraction (XRD). The microstructure and magnetic properties were investigated by means of a scanning electron microscope (SEM) and vibrating sample magnetometer (VSM), respectively. Structural transformation from rhombohedral in pure BF to mixed-phase between rhombohedral and tetragonal when added with 50 wt% PT has been revealed from XRD analysis. The magnetic properties are generally seen to reduce with an increase in the content of the PT phase. Interestingly, the M-H hysteresis loop measurements indicated that the composites exhibited superparamagnetic behavior at room temperature for all compositions, a noticeable contradiction to the magnetic behavior earlier reported for the BF-PT solid-solution.

1 Introduction

In recent years, there has been an increasing interest in multiferroic materials, which combine two or more of the properties of ferromagnetism, ferroelectricity, and ferroelasticity. Coupling between magnetic and electric ordering leads to magnetoelectric (ME) effect [1, 2]. These compounds present opportunities for potential applications in information storage, the emerging field of spintronics, sensors, and multistate memory devices [3, 4]. The ME phenomenon is observed in both single-phase [1, 5] as well as composite [6, 7] materials. The utilization of single phase ME materials in particular device applications is limited due to very low ME effect at room temperature [8, 9]. On the other hand, composite materials that consist of different ceramic phases with different electrical/ferroelectric/magnetic properties reveal an excellent magnetoelectric coefficient [6, 7]. It is supposed that two kinds of electronic ceramics are incorporated into one material, which might present various effects, such as the sum effect and the product effect [10].

Keywords Multiferroic · Composites · BiFeO3-based

ceramics - Perovskite - Magnetic properties

Studies on ME composites were initiated in the early 1970s by Boomgaard et al. [11, 12] on ferromagnetic spinel and barium titanate. At present, various composites have been reported in literature such as Ni(Co,Mn)Fe2O4-BaTiO<sub>3</sub> [11], CoFe<sub>2</sub>O<sub>4</sub>-BaTiO<sub>3</sub> [13], NiFe<sub>2</sub>O<sub>4</sub>-PZT [14], CuFc<sub>2</sub>O<sub>4</sub>-PZT [15], and Ni<sub>0.93</sub>Co<sub>0.02</sub>Mn<sub>0.05</sub>Fe<sub>1.95</sub>O<sub>4</sub>-Na<sub>0.5</sub>Bi<sub>0.5</sub>TiO<sub>3</sub> (NMF-NBT) [7]. Since the ME output in these composite materials is found to be high, they are deemed useful for electronic applications. Most of these materials use BaTiO3 and PZT as the ferroelectric phase or spinel ferrite as the magnetic phase. However, there is

R, Wongmaneerung ( )

Faculty of Science, Maejo University, Chiang Mai 50290,

e-mail: re\_nok@yahoo.com

P. Jantaratana

Department of Physics, Kasetsart University, Bangkok 10900, Thailand

R. Yimnirun

School of Physics, Suranaree University of Technology, Nakhon Ratchasima 30000, Thailand

Department of Physics and Materials Science, Faculty of Science, Chiang Mai University, Chiang Mai 50200, Thailand

Fig. 1 XRD patterns of (1-x)BF-xPT multiferroic composites sintered at 800 °C with (a) 0, (b) 10, (c) 20, (d) 30, (e) 40, (f) 50, and (g) 100 wt% of PT

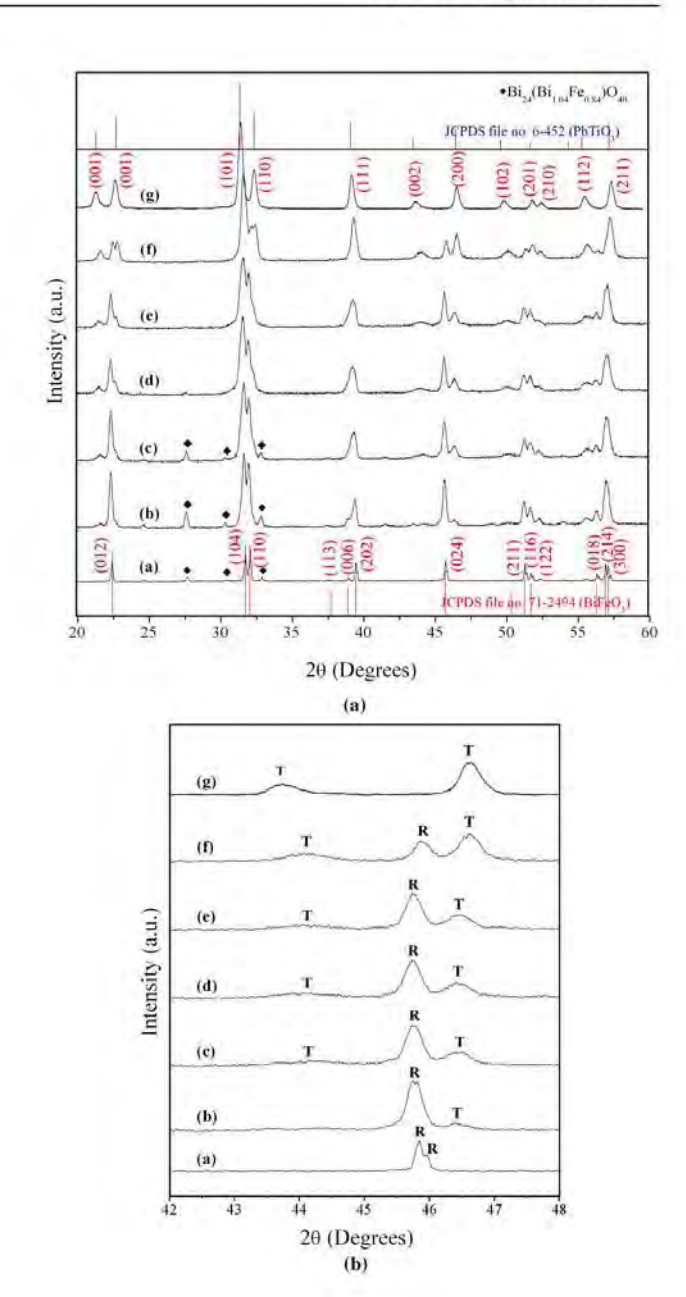
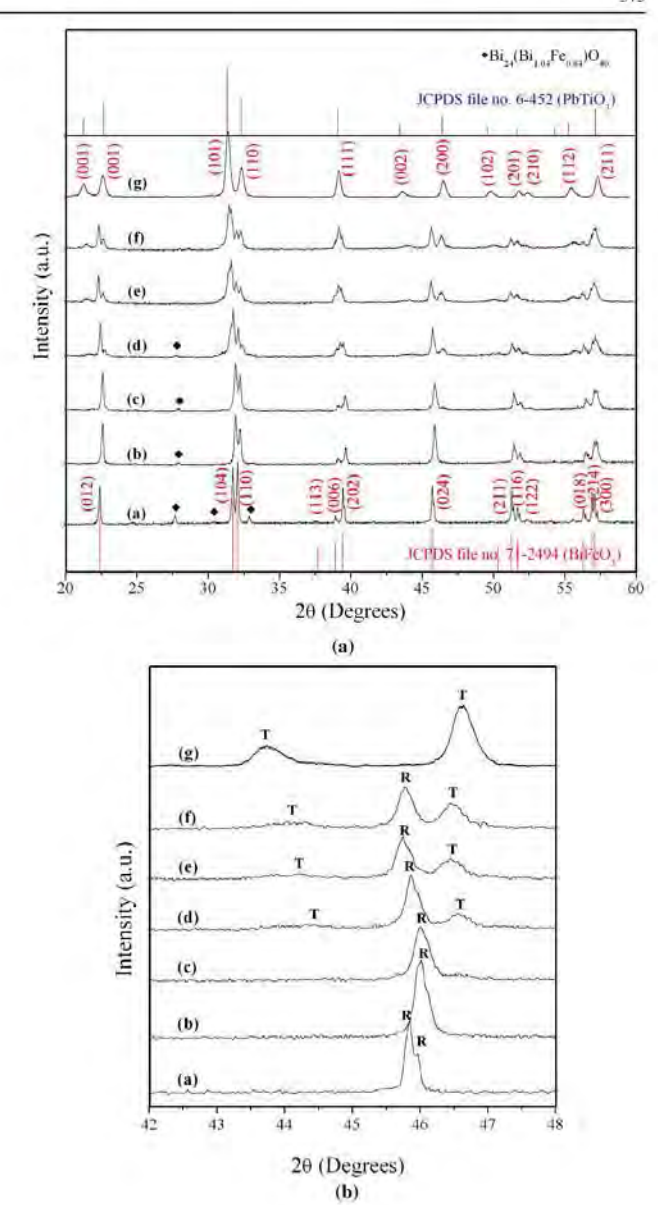




Fig. 2 XRD patterns of (1-x)BF-xPT multiferroic composites sintered at 900 °C with (a) 0, (b) 10, (c) 20, (d) 30, (e) 40, (f) 50, and (g) 100 wt% of PT



a very limited use of  $BiFeO_3$  or perovskite ferrite combined with the ferroelectric phase in multiferroic composite materials. The perovskite  $BiFeO_3\ (BF)$  is one of the

few known ferroelectromagnetic (FEM) multiferroic with both ferroelectric ( $T_{\rm C}=830~^{\circ}{\rm C}$ ) [16] and antiferromagnetic ( $T_{\rm N}=370~^{\circ}{\rm C}$ ) [17], which was expected to be accompa-



nied by a large spontaneous polarization ( $\sim 100~\mu C/cm^2$ ). It shows a distorted perovskite structure with rhombohedral symmetry and shows a weak ferro/ferromagnetic characteristic in some temperature ranges [18, 19].

Nonetheless, one of the major problems of BF is its low electrical resistivity. Currently, two methods are used to solve the problem: one is to add some dopants such as gallium [20] and tantalum [21] to improve the properties, and the other is to add perovskites such as PbTiO<sub>3</sub> (PT), BaTiO<sub>3</sub> (BT), and SrTiO<sub>3</sub> (ST) [20, 22] into a solid–solution with BF in order to stabilize a perovskite structure and enhance electrical resistivity. In BF-PT solid solutions, the spontaneous moment was observed even up to very high temperatures [23]. The values of specific magnetic moment observed for various concentrations of Bi-FeO<sub>3</sub> in the BF-PT system varied between 0.017 and 0.004 G cm<sup>3</sup>/g at room temperature.

These results lead to the assumption that a system with a similar structure and physical property variations should also show spontaneous magnetic moment [24]. However, the MPB BF-PT compositions show high tetragonality, making the sintered bodies crack during cooling due to high internal stress or during domain switching under a high defield. Based on the authors' work [25], the idea of ceramic a nanocomposite approach could be applied to other perovskite ferroelectric materials such as BF-PT. Thus, this study deals with work carried out to fabricate ceramic. Furthermore, no work on the ME composites based on BF is reported in the literature. In the present study, BF was closen as the magnetic phase to prepare the ME composite with ferroelectric PT. This paper reports the phase formation behavior of BF-PT composites and their magnetic properties.

#### 2 Experimental Procedure

The constituents of multiferroic composites namely, ferromagnetic and ferroelectric phases, were prepared separately by the solid-state sintering method. The ferrite BiFeO<sub>3</sub> (BF) was produced by ball-milling precursors of high-purity basic oxide Bi<sub>2</sub>O<sub>3</sub> (99.99 %, Aldrich) and Fe<sub>2</sub>O<sub>3</sub> (99.99 %, Aldrich) in ethanol for 24 h followed by calcination at 800 °C for 4 h [26]. The calcined BF powders were ground thoroughly. Laboratory-grade powders of PbO (99.99 %, Fluka) and TiO<sub>2</sub> (99.99 %, Riedel deHaen) were used as starting materials to synthesize the ferroelectric PbTiO<sub>3</sub> (PT). The powders were taken in the stoichiometric ratio and the mixture was calcined at 600 °C for 2 h in air [27].

After calcining, the X-ray diffraction analysis showed that  $BiFeO_3$  and  $PbTiO_3$  phases were formed. These two starting powders were then utilized to prepare the multiferroic composites with the nominal composition of (1-x)BF-xPT, where the weight fraction (x) of PT was 0.1, 0.2, 0.3,

Table 1 Physical properties of (1-x)BF-xPT multiferroje composites

Sintering temperature (°C for 2 h)	Composition (x)	Density <sup>a</sup> (g/cm <sup>3</sup> )	Grain size <sup>b</sup> (µm)	
			BF grain	PT grain
800	0.1	7,652	2,00-3.55	0.11-0.28
	0.2	7.649	2.67-5.70	0.25-0.33
	0.3	7.640	2.60-5.40	0.20-0.34
	0.4	7,618	3.00-5.40	0.20-0.30
	0,5	7.556	2.60 4.40	0.20-0,40
900	0.1	7.722	3.40-7.40	0.20-0.30
	0.2	7.711	4.20-7.00	0.24-0.40
	0.3	7,645	5.00-5.00	0.20-0.40
	0.4	7.676	3.80-5.60	0.30-0.42
	0.5	7.677	3.80-6.20	0.30-0.40

<sup>&</sup>lt;sup>a</sup>The estimated precision of the density is ±0.05 g/cm<sup>3</sup>

0.4, and 0.5. The composite powders were added with 3 % polyvinyl alcohol as a binder and pressed into pellets having a 1.5 mm thickness and 10 mm diameter. After binder burnout at 500 °C for 1 h, sintering of the samples was performed between 750–900 °C for 2 h and cooled in the furnace. X-ray diffraction (XRD; Siemens-D500 diffractometer) was carried out at room temperature using Cu K $\alpha$  radiation to identify the phase formed. The microstructural development was characterized using a scanning electron microscopy (SEM; JEOL JSM-840A). Grain sizes of the sintered ceramics were directly estimated from the SEM micrographs. Magnetic hysteresis loops were obtained at room temperature on the composites using a vibrating sample magnetometer (VSM) at room temperature.

#### 3 Results and Discussion

Figures 1 and 2 show the X-ray diffraction (XRD) patterns for (1-x)BF-(x)PT (x = 0.1, 0.2, 0.3, 0.4, and 0.5) composites with sintering temperature at 800 and 900 °C for 2 h, respectively. The strongest reflections in the majority of XRD traces clearly reflect the characteristic of both BiFeO3 (ferrite) and PbTiO3 (ferroelectric) phases which could be matched with JCPDS files no. 71-2494 and 6-452, respectively. All the peaks can be indexed and there are no unidentified peaks indicating the absence of a chemical reaction between the two phases. However, a considerable amount of Bi24(Bi1 04Fe0 84)O40 was formed. This indicates the chemical reaction between Bi2O3 and Fe2O3 during the BiFeO3 formation process. The individual BiFeO3 (BF) and PbTiO3 (PT) phases stabilize in rhombohedral and tetragonal structures, respectively [28, 29]. In these composites from both sintering conditions, the characteristic peak of PT increases



<sup>&</sup>lt;sup>b</sup>The estimated precision of the grain size is  $\pm 0.05$  g/cm<sup>3</sup>

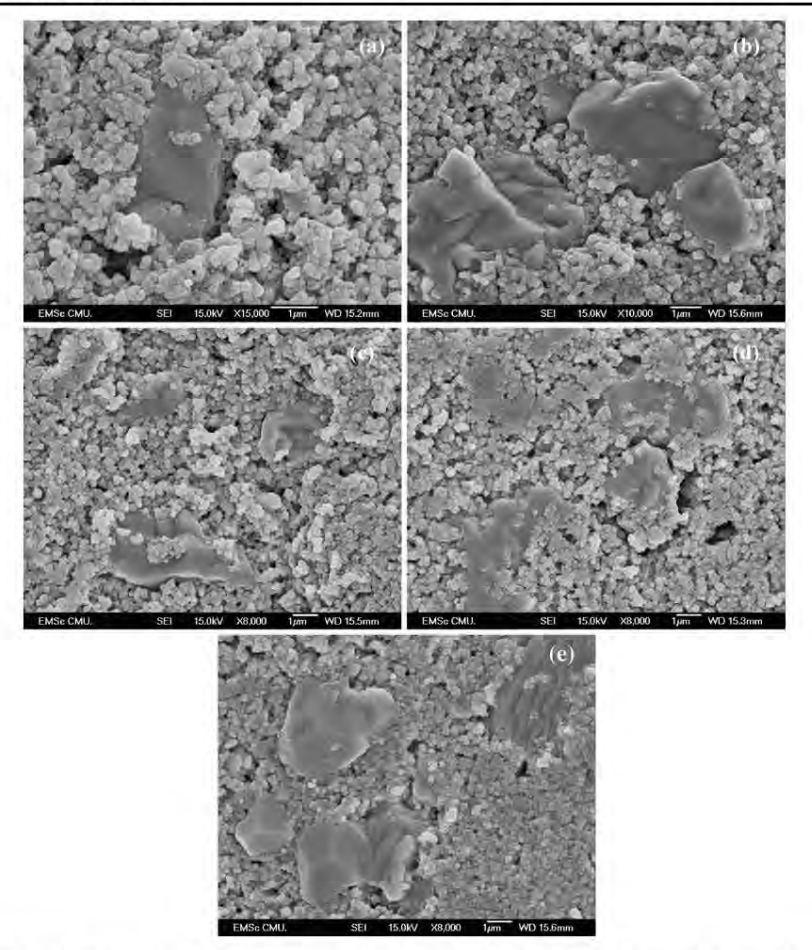


Fig. 3 SEM micrographs of (1-x)BF-xPT multiferroic composites sintered at 800 °C with (a) 10, (b) 20, (e) 30, (d) 40, and (e) 50 of PT

with the increasing content of PT, whereas the characteristic peak of ferrite decreases.

More interestingly, at a lower sintering temperature (800 °C), the mixture of BF and PT phases (composite characteristic) can be noticed at x=10 %wt, whereas the samples sintered at a higher temperature show a clear mixture of phases at x=30 %wt. This may be due to the fact that the high sintering temperature provides sufficient energy to produce solid–solution ceramics, rather than forming composites, in low PT content compositions. For example, the diffraction line around  $2\theta$  of  $42-48^\circ$  is shown in Figs. 1(b) and 2(b) confirming their rhombohedral and tetragonal sym-

metries. Moreover, when comparing these results with the solid-solution system in previous work [30], it is found that diffraction patterns of 0.9BF-0.1PT solid-solution exhibited a rhombohedral phase, whereas 0.7BF-0.3PT crystallized in a mixture of tetragonal and rhombohedral phases. However, in those cases, high sintering temperatures of 1015, 1020, and 1025 °C were employed.

Sample density was measured by the Archimedes method. Densification was promoted with increasing sintering temperature and subsequently reached a maximum density at 900 °C for all compositions, as shown in Table 1. The density values increased slightly with the increasing content



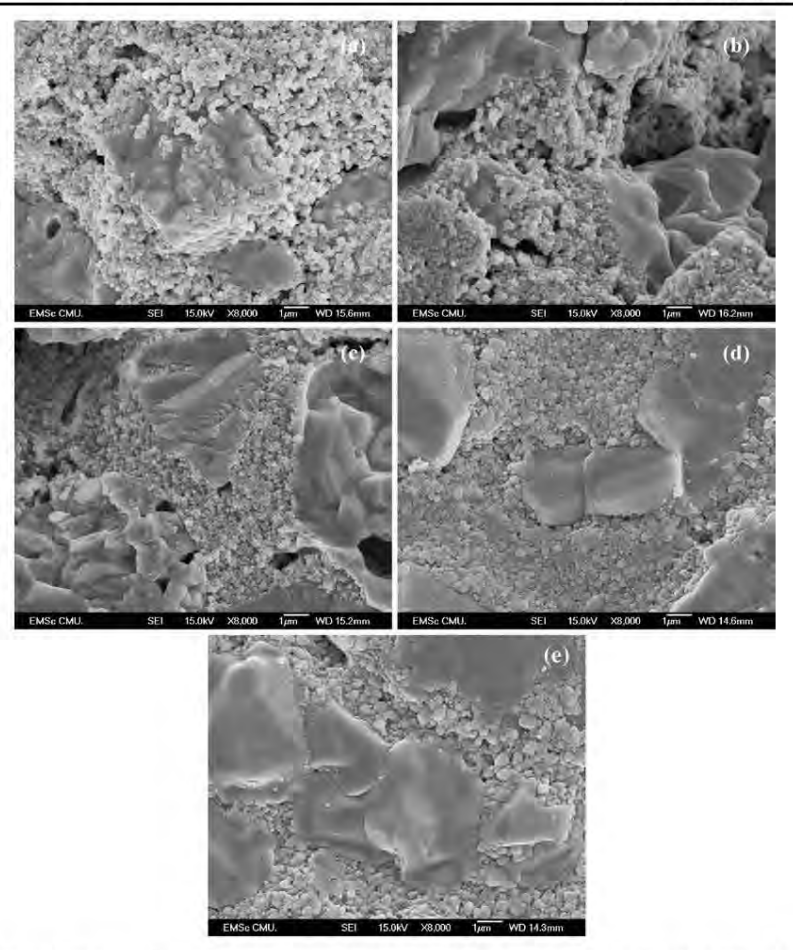


Fig. 4 SEM micrographs of (1-x)BF-xPT multiferroic composites sintered at 900 °C with (a) 10, (b) 20, (e) 30, (d) 40, and (e) 50 of PT

of the PT phase. The higher densities may be attributed to the employed bimodal particle size method via both geometric interlocking and improved cohesion between particles. However, the density decreased with PT content when sintered at 800 °C. This decrease in density seems to be mainly due to the dissolution or interdiffusion between the BF and PT phases, as seen in the XRD patterns and SEM micrographs. In addition, large pores may be the reason for this decrease in density. This limitation of the densification due to large pores, also found in other systems [31, 32], might have been formed by the stress caused by heterogeneities of the sintering rate between BF and PT.

SEM investigation performed on the surface of the BFPT composites sintered at 800 °C and 900 °C are compared in Figs. 3 and 4, respectively. In general, SEM micrographs pointed out a heterogeneous microstructure with bimodal grain size distribution, consisting of large grains (BF grains) with an equivalent average size of  $\sim\!4.6~\mu m$ , and small PT grains with a size in the range of 0.2–0.4  $\mu m$ . Moreover, the micrographs demonstrate that these composites possess high density and well-defined grains. The grains of BF and PT are distributed homogeneously. In these figures, ferrite grains appear as a dark color, where as PT grains appear with a light color.



Fig. 5 M-H hysteresis loops of (1-x)BF-xPT multiferroic composites sintered at  $800~^{\circ}C$ 

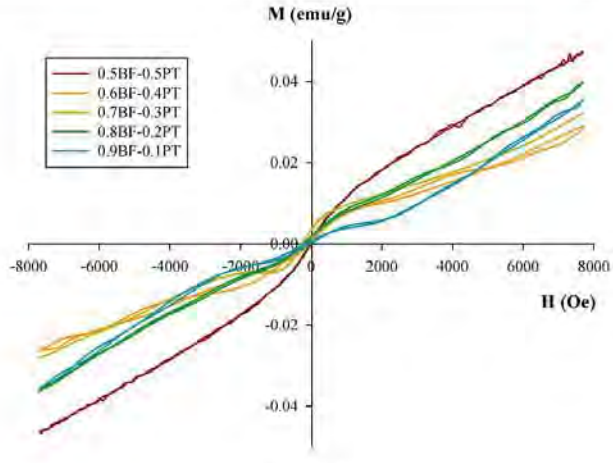
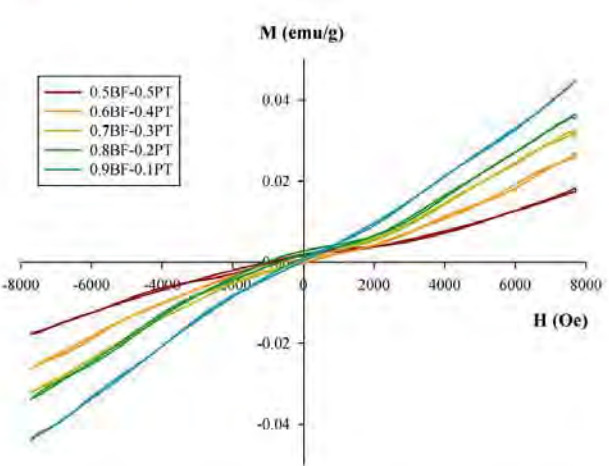


Fig. 6 M-H hysteresis loops of (1-x)BF-xPT multiferroic composites sintered at 900 °C



The SEM observations clearly confirm the XRD results and indicate the successful formation of BF–PT composites. As indicated by the XRD patterns, the SEM microstructures of the composites did not show any third phase caused by a chemical reaction or interdiffusion between the two phases. However, there are some large pores compared with the PT grain size. These poorly sintered samples could be attributed to several factors, including the effect of ineffective mixing or low firing temperature, similar to those observed by other researchers [33, 34]. Moreover, it should be noted that the radius of Pb<sup>2+</sup> is larger than that of Bi<sup>3+</sup>, while the radius of Ti<sup>4+</sup> is smaller than that of Fe<sup>3+</sup>. Therefore, the possibility of ions substitution should not be the case, since no sufficient ionization or diffusion can be expected.

Figures 5 and 6 show the room temperature M-H hysteresis loops for (1-x)BF-xPT composites sintered at 800 and 900 °C, respectively, at fields of less than 8000 Oc. The magnetic properties of all composites show very interesting features. There is no remanent magnetization and coercivity. For x=0.1, the saturation magnetization is 0.035 (0.045) emu/g, and for x=0.2,0.3,0.4 and 0.5, the values of 0.040 (0.037), 0.032 (0.033), 0.029 (0.026), and 0.047 (0.018) emu/g were obtained, respectively, when samples were sintered at 800 °C (900 °C) as displayed in Table 2. This indicated that the saturation magnetization decreased with increasing PT content. These values are smaller than the value of  $\sim 0.2$  emu/g for pure BF [30]. It should be attributed to the influence of the pinning effect of the non-



Table 2 Magnetic properties of (1 x)BF xPT multiferroic compos-

Sintering temperature (°C for 2 h)	Composition (x)	Magnetic properties		
		Ms (emu/g)	M <sub>r</sub> (emu/g)	Coercivity (Oe)
800	0.1	0.035	-	-
	0.2	0.040	-	2
	0,3	0,032	-	0
	0.4	0.029	-	-
	0.5	0,047	-	-
900	0.1	0.045	-	=
	0.2	0.037	-	0
	0.3	0.033	-	8
	0.4	0.026	-	-
	0.5	0.018	-	8
825 °C for 20 min [33]	0.1	0.225	0.040	132
	0.3	0.210	0.016	76

magnetic phase PT, as also reported in PbTiO3/NiFe2O4 composites [35].

It should be mentioned here that the M-H loops at room temperature exhibit superparamagnetic behavior. In the case of a solid solution [30], the magnetic hysteresis loops show that the antiferromagnetic behavior of BF (linear M(H) dependence) is turned into a weak ferromagnetic state by the addition of PT. Room temperature superparamagnetism in BF-PT composites completely differs from the linear M-H relationship in the BF-PT solid solution. If the material is nonhomogeneous, one can observe a mixture of ferromagnetic and paramagnetic clusters of atoms at the same temperature that is the superparamagnetic stage [36]. In this case, the differences between BF and PT are that one is (anti)ferromagnetic (BF) and the other is paramagnetic; hence, the superparamagnetism phenomenon can occur. Moreover, ferromagnetic materials undergo a transition to a paramagnetic state above its Curie temperature, whereas superparamagnetism differs from this standard transition, since it occurs below the Curie temperature of the material [37].

#### 4 Conclusions

The two-phase multiferroic composites containing ferrite and ferroelectric phases have been synthesized by the solidstate sintering technique. The coexistence of BF and PT phases in these composites has been confirmed from the XRD analysis and SEM images. All the composites reveal magnetic hysteresis loops, showing superparamagnetic behavior, and the saturation magnetization values are found to decrease with increasing PT content.

Springer

Acknowledgements The authors would like to thank the Thailand search Fund (TRF) and Faculty of Science of Maejo University for their financial support. Also acknowledged for additional technical support is the Processing Technology of Materials Research Laboratory (PTMRL).

#### References

- 1. Eerenstien, W., Mathur, N.D., Scott, J.F.: Nature 442(17), 759
- Smolenskii, G.A., Chupis, L. Sov. Phys. Usp. 25, 475 (1982)
- Wang, J., Neaton, J.B., Zheng, H., Nagarajan, V., Ogale, S.B., Liu, B., Viehland, D., Vaithyanathan, V., Schlom, D.G., Waghmare, U.V., Spaldin, N.A., Rabe, K.M., Wutting, M., Ramesh, R.: Science 299, 1719 (2003)
- Fiebig, M., Lottermoser, T., Frohlich, D., Goitsev, A.V., Pisarev. R.V.: Nature 419(6909), 818 (2002)
- Woodward, D.I., Reancy, I.M., West, A.R., Randall, C.A.: J. Appl. Phys. 94(5), 3313 (2003)
- Yu, Z., Ang, C.: J. Mater, Sci. 13, 193 (2002) Babu, S.N., Srinivas, K., Bhimasankaram, T.: J. Magn. Magn. Mater. 321, 3764 (2009)
- Ryu, J., Carazo, A.V., Uchino, K., Kim, H. E., Jpn. J. Appl. Phys. 40, 4948 (2001)
- Islam, R.A., Priya, S.: Integr. Ferroelectr. 82, 1 (2006)
- Newnham, R.E.: Annu. Rev. Mater. Sci. 16, 47 (1986)
- Van Den Boomgaard, J., Terrell, D.R., Born, R.A.J.: J. Mater. Sci. 9, 1705 (1974)
- Van Den Boomgaard, J., Born, D.R. Terrell R.A.J.: J. Mater. Sci. 13, 1538 (1978)
- Harshe, G., Dougherty, J.P., Newnham, R.E.: Int. J. Appl. Electromagn. Mater. 4, 161 (1993)
- Zhai, J., Cai, N., Shi, Z., Lin, Y., Nan, C.-W.; J. Phys. D, Appl. Phys. 37, 823 (2004)
- Dai, Y.R., Bao, P., Wan, J.S., Shen, H.M., Liu, J.M.: J. Appl. Phys. 96, 5687 (2004)
- Smolenskii, G.A., Isupov, V., Agranovskaya, A., Krainik, N.: Sov. Phys., Solid State 2, 2651 (1961)
- Morean, J.M., Michel, C., Gerson, R., James, W.J.: J. Phys. Chem. Solids 32, 1315 (1971)
- Neaton, J.B., Ederer, C., Waghmare, U.V., Spaldin, N.A., Rabe, K.M.: Phys. Rev. B 71, 014113 (2005)
- Ricinschi, D., Yun, K.Y., Okuyama, M.: J. Phys. Condens. Matter 18 1.97 (2006)
- Cheng, J.R., Li, N., Cross, L.E.: J. Appl. Phys. 94, 5153 (2003)
- Mathe, V.L., Patankar, K.K., Patila, R.N., Lokhande, C.D., J. Magn. Magn. Mater. 270, 380 (2004)
- Kumar, M.M., Srinivas, A., Suryanarayana, S.V.: J. Appl. Phys. 87, 855 (2000)
- Fedulov, S.A., Ladyzhinskii, P.B., Pyatigorskaya, I.L., Venevtsev, Yu.N.: Sov. Phys., Solid State 6, 375 (1964)
- Kumar, M.M., Srinath, S., Kumar, G.S., Suryanarayana, S.V.: J. Magn. Magn. Mater. 188, 203 (1998)
- Wongmaneerung, R., Rujiwatra, A., Yimnitun, R., Ananta, S.: J. Alloys Compd. 475, 473 (2008)
- Silawongsawat, C., Chandarak, S., Sareein, T., Ngamjarurojana, A., Maensiri, S., Laoratanakul, P., Ananta, S., Yimnirun, R., Adv. Mater. Res. 55-57, 237 (2008)
- Wongmaneerung, R., Yimnirun, R., Ananta, S.: Mater. Lett. 60, 2666 (2006)
- Jia, D.-C., Xu, J.-H., Ke, H., Wang, W., Zhou, Y.: J. Eur. Geram. Soc. 29, 3099 (2009)
- Wongmaneerung, R., Yimnirun, R., Ananta, S.: Appl. Phys. A 86, 249 (2007)

- Singh, K., Negi, N.S., Kotnala, R.K., Singh, M.: Solid State Commun. 148, 18 (2008)
   Wongmaneerunga, R., Singjai, P., Yimnirun, R., Ananta, S.: J. Alloys Compd. 475, 456 (2009)
   Wongmaneerung, R., Choopan, S., Yimnirun, R., Ananta, S.: J. Alloys Compd. 509, 3547 (2011)
   Wongmaneerung, R., Yimnirun, R., Ananta, S.: J. Mater. Sci. 44, 5428 (2009)

- Zhang, J., Wang, L., Shi, L., Jiang, W., Chen, L.: Scr. Mater. 56, 241 (2007)
- Zhu, L., Dong, Y., Zhang, X., Yao, Y., Weng, W., Han, G., Ma, N., Du, P. J. Alloys Compd. 503, 426 (2010)
   Tilley, R.: Understand Solids—The Science of Materials, pp. 383–384. Wiley, Chichester (2004)
- 37. Néel, L.: Ann. Geophys. 5, 99 (1949)



## Manuscript ที่ได้จัดส่งวารสาร Materials Chemistry and Physics

Elsevier Editorial System(tm) for Materials Chemistry and Physics Manuscript Draft

Manuscript Number:

Title: Phase Formation, Dielectric and Magnetic Properties of Bismuth Ferrite-Lead Magnesium Niobate Multiferroic Composites

Article Type: Full Length Article

Keywords: Multiferroic; composites; BiFeO3-based ceramics; magnetic properties

Corresponding Author: Miss Rewadee Wongmaneerung, Ph.D.

Corresponding Author's Institution:

First Author: Rewadee Wongmaneerung, Ph.D.

Order of Authors: Rewadee Wongmaneerung, Ph.D.; Jintara Padchasri; Rungnapa Tipakontitikul, Ph.D.; Pongsakorn Jantaratana, Ph.D.; Rattikorn Yimnirun, Ph.D.; Supon Ananta, Ph.D.

Abstract: Binary multiferroic composites (1-x)BiFeO3-xPb(Mg1/3Nb2/3)O3 (BF-PMN; x = 0.0-50 wt%) were fabricated by a traditional ceramic process. The effect of PMN contents on phase assemblage, microstructure, dielectric and magnetic properties of the samples were investigated by X-ray diffraction (XRD), scanning electron microscope (SEM), LCR meter and vibrating sample magnetometer (VSM), respectively. The results indicate that all composites show the perovskite structure and PMN phase is compatible with BF phase. The microstructure display the mix phases between BF, PMN, Bi-rich BF and Fe-rich BF phases. Dielectric anomalies of these composites are totally different from BiFeO3 single phase. Moreover, dielectric constant is found to be increased as the content of PMN decrease. Magnetic transition temperatures are in the range of 270-440 oC. Interestingly, the M-H hysteresis loop measurements indicated that all composites exhibited weak ferromagnetism behavior at room temperature. The maximum remanent magnetization Mr is observed for x = 30 wt% and then decreases with PMN contents is more than 40 wt%.

Suggested Reviewers: Xiaoli Tan Ph.D.
Associate Professor, Materials Science and Engineering, Iowa State University xtan@iastate.edu

Helen Chan Ph.D. Materials Science and Engineering, Lehigh University Helen.Chan@lehigh.edu

David Cann Ph.D. Oregon State University cann@engr.orst.edu

Opposed Reviewers:

#### Rewadee wongmaneerung

Materials Science Program, Faculty of Science Maejo University Chiang Mai 50290 THAILAND E-mail: re\_nok@yahoo.com

Jan 03, 2013

Dear Editor;

Enclosed please an original manuscript being submitted for publication in Materials Chemistry and Physics. The manuscript is detailed as follow:

#### Title: Phase Formation, Dielectric and Magnetic Properties of Bismuth Ferrite-Lead Magnesium Niobate Multiferroic Composites

Author: R. Wongmaneerung, J. Padchasri, R. Tipakontitikul, P. Jantaratana, R. Yimnirun and S. Ananta

Institution: 1. Materials Science Program, Faculty of Science, Maejo University, Chiang Mai, 50290, Thailand

> Department of Physics, Ubonratchathani University, Ubonratchathani 31490, Thailand

3. Department of Physics, Kasetsart University, Bangkok 10900, Thailand

 School of Physics, Institute of Science, Suranaree University of Technology, Nakhon Ratchasima 30000, Thaialnd

 Department of Physics and Materials Science, Faculty of Science, Chiang Mai University, Chiang Mai 50200, Thailand

Keywords: Multiferroic; composites; BiFeO3-based ceramics; magnetic properties

This article describes Binary multiferroic composites (1-x)BiFeO<sub>3</sub>-xPb $(Mg_{1/3}Nb_{2/3})O_3$  (BF-PMN; x = 0.0–50 wt%) were fabricated by a traditional ceramic process. The effect of PMN contents on phase assemblage, microstructure, dielectric and magnetic properties of the samples were investigated by X-ray diffraction (XRD), scanning electron microscope (SEM), LCR meter and vibrating sample magnetometer (VSM), respectively. The results indicate that all composites show the perovskite structure and PMN phase is compatible with BF phase. The microstructure display the mix phases between BF, PMN, Bi-rich BF and Fe-rich BF phases. Dielectric anomalies of these composites are totally different from BiFeO<sub>3</sub> single phase. Moreover, dielectric constant is found to be increased as the content of PMN decrease. Magnetic transition temperatures are in the range of 270–440 °C. Interestingly, the M-H hysteresis loop measurements indicated that all composites exhibited weak ferromagnetism behavior at room temperature. The maximum remanent magnetization  $M_t$  is observed for x = 30 wt% and then decreases with PMN contents is more than 40 wt%.

Thank you very much for your valuable time and very kind consideration. Should you have any questions regarding the manuscript, please feel free to contact me. I would really appreciate if

you could inform me of the status of the manuscript. I am looking forward to hearing from you very soon.

## Sincerely yours,

Rewadee Wongmancerung Materials Science Program, Faculty of Science, Maejo University, Chiang Mai, 50290, Thailand E-mail: re\_nok@yahoo.com

#### \*Highlights (for review)

## Research Highlights

A bimodal particle size concept was designed in the production of BF-PMN composites.

A very abnormal diffuse dielectric pattern is observed during the heating process.

BF-PMN composites show highly saturated magnetization.

# Phase Formation, Dielectric and Magnetic Properties of Bismuth Ferrite-Lead Magnesium Niobate Multiferroic Composites

R. Wongmaneerung11, J. Padchasri2, R. Tipakontitikul2, P. Jantaratana3, R. Yimnirun4 and S. Ananta5

<sup>1</sup>Faculty of Science, Maejo University, Chiang Mai 50290, Thailand

<sup>2</sup> Department of Physics, Ubonratchathani University, Ubonratchathani 31490, Thailand

<sup>3</sup>Department of Physics, Kasetsart University, Bangkok 10900, Thailand

School of Physics, Institute of Science, Suranaree University of Technology, Nakhon Ratchasima 30000, Thaialnd

<sup>5</sup>Department of Physics and Materials Science, Faculty of Science, Chiang Mai University,

Chiang Mai 50200, Thailand

#### Abstract

Binary multiferroic composites (1-x)BiFeO<sub>3</sub>-xPb(Mg<sub>1/3</sub>Nb<sub>2/3</sub>)O<sub>3</sub> (BF-PMN; x = 0.0–50 wt%) were fabricated by a traditional ceramic process. The effect of PMN contents on phase assemblage, microstructure, dielectric and magnetic properties of the samples were investigated by X-ray diffraction (XRD), scanning electron microscope (SEM), LCR meter and vibrating sample magnetometer (VSM), respectively. The results indicate that all composites show the perovskite structure and PMN phase is compatible with BF phase. The microstructure display the mix phases between BF, PMN, Bi-rich BF and Fe-rich BF phases. Dielectric anomalies of these composites are totally different from BiFeO<sub>3</sub> single phase. Moreover, dielectric constant is found to be increased as the content of PMN decrease. Magnetic transition temperatures are in the range of 270–440 °C. Interestingly, the M-H

\*Corresponding author: Tel.: 66 53 873515; fax: 66 53 878225

E-mail address: re\_nok@yahoo.com (R. Wongmaneerung)

hysteresis loop measurements indicated that all composites exhibited weak ferromagnetism behavior at room temperature. The maximum remanent magnetization  $M_{\rm r}$  is observed for x=30 wt% and then decreases with PMN contents is more than 40 wt%.

Keywords: Multiferroic; composites; BiFeO3-based ceramics; magnetic properties

#### 1. Introduction

Materials that have coupled electric, magnetic and structural order parameters that result in simultaneous ferroelectricity, ferromagnetism and ferroelasticity are known as multiferroics [1, 2]. Most of solid-solution or single-phase ferroelectric-magnetic materials have few applications due to their low Néel temperature (TN) or Curie temperature (TC) except some materials such as BiFeO3 (BF). The perovskite BF is ferroelectric (T<sub>C</sub> ~830 °C) and antiferromagnetic ( $T_N$  ~370  $^{\circ}$ C) and shows a weak ferro/ferrimagnetic in some temperature ranges [3-5]. However, composite multiferroic materials have received considerable attention in recent years. Various multiferroic composites that consist of different ceramic phases with different electrical/ferroelectric/magnetic properties have been studied [6-8]. Not only the physical mechanism of ferroelectric/ferromagnetic composite but also its potential application in microelectronic devices was investigated. For example, the ferroelectric ceramic BaTiO3 has the piezoelectric effect [9] and the ferromagnetic ceramic CoFe<sub>2</sub>O<sub>4</sub> has the piezomagnetic effect [10]. When the composite materials were prepared, an electric-magnetic coupling effect occurred and an excellent magnetoelectric coefficient was reported [7]. One more sample, BF exhibits characteristic features in dielectric properties around the magnetic transition temperature [11]. PbTiO<sub>3</sub> (PT) exhibits the most desirable dielectric, piezoelectric and pyroelectric properties for high frequency and temperature applications [12, 13]. The coexistence of these two compounds reveals magnetic hysteresis

loops, showing superparamagnetic behavior [14]. If two compounds can be successfully incorporated into a composite [6–14], it is expect that the composite might have interesting electrical/magnetic properties, which may find potential applications. Nevertheless, most of these high performance materials use BaTiO<sub>3</sub>, PbTiO<sub>3</sub> and Pb(Zr,Ti)O<sub>3</sub> as ferroelectric or piezoelectric phase. Recently, the electromagnetic properties of the composite ceramics of NiFe<sub>2</sub>O<sub>4</sub>–Ba<sub>8</sub>Sr<sub>y</sub>TiO<sub>3</sub> [15–17] have been reported and showed the good dielectric and magnetic properties. However, to our knowledge, the use of relaxor ferroelectric Pb(Mg<sub>1/3</sub>Nb<sub>2/3</sub>)O<sub>3</sub> phase with magnetic phase to fabricate multiferroic composites has not been reported so far. Pb(Mg<sub>1/3</sub>Nb<sub>2/3</sub>)O<sub>3</sub> or PMN is one of the most widely investigated perovskite relaxor ferroelectric materials, because of its high dielectric constant and electrostrictive coefficient [18, 19]. Therefore, this study deals with work carried out to fabricate multiferroic composite in the BF/PMN system. The relationships between phase formation, microstructure, dielectric and magnetic properties of these materials will be established.

#### 2. Experimental Procedure

The components of the ceramic composites were chosen as ferrite BF and relaxor ferroelectric PMN. They were prepared separated by solid–state reaction. The ferrite BF was produced by ball–milling precursors of high–purity basic–oxide Bi<sub>2</sub>O<sub>3</sub> (99.99%, Aldrich) and Fe<sub>2</sub>O<sub>3</sub> (99.99%, Aldrich) in ethanol for 24 h followed by calcination at 800 °C for 4 h [14]. PMN powders were synthesized by employing B–site corundum precursor mixed oxide synthetic route [20]. First, intermediate phase of magnesium niobate: Mg<sub>4</sub>Nb<sub>2</sub>O<sub>9</sub> was prepared by conventional method. The appropriate amount of PbO was then added to the Mg<sub>4</sub>Nb<sub>2</sub>O<sub>9</sub> and ball–milled in ethanol for 24 h. Corundum–route mixtures were calcined at

950 °C for 1 h. In the BF-PMN mixing process, these two types of powders were utilized to prepare the multiferroic composites with the nominal composition of (1-x)BF-xPMN, where the weight fraction (x) of PMN was 0, 10, 20, 30, 40 and 50 wt%, respectively. The calculated relevant proportions were suspended in ethanol and intimately mixed in a ball-mill, Drying was carried out and ground into the fine powders. The composite powders were added 3% polyvinyl alcohol as binder and pressed into pellets having 1-2 mm thickness and 10 mm diameter. These pellets were sintered in air at 800-900 °C for 2 h and cooled in the furnace.

X-ray diffraction (XRD; Siemens–D500 diffractometer) was carried out at room temperature using Cu  $K_{\alpha}$  radiation to identify the phase formed. The microstructural development was characterized using a scanning electron microscopy (SEM; JEOL JSM-840A). Grain sizes of the sintered ceramics were directly estimated from the SEM micrographs. For electric and dielectric measurement both surface of pellets were polished and coated with silver paste to make electrodes. Dielectric constant and dielectric loss were studied by Precision LCR meter 4285A in frequency range 10 kHz -1 MHz. Magnetic measurement is performed using vibrating sample magnetometer (VSM) at room temperature.

#### 3. Results and Discussion

The X-ray diffraction patterns obtained from (1-x)BF-xPMN (x = 0-50 wt%) multiferroic composites sintered at 800 and 900 °C are displayed in Figs. 1 and 2, respectively, where the perovskite structure was formed throughout the whole composition ranges. The patterns clearly reflect the characteristic of both BF and PMN phases which could be matched with JCPDS file no. 71–2494 and 81–861, respectively. For all investigated

composites, perovskite structure of rhombohedral R3c symmetry was identified, with a gradual attenuation of the rhombohedral distortion with PMN content increasing. This tendency to a gradual change towards a cubic symmetry with the PMN addition is proved by the cancellation of the splitting of the XRD (104), (006), (202), (116), (122), (214) and (303) maxima specific of pure BF, as observed in the detailed representation from Figs. 1 and 2. This result is similar with (1-x)BF-xBT system that was pointed out by F. Prihor *et al.* [21]. However, a considerable amount of  $Bi_{24}(Bi_{1.04}Fe_{0.84})O_{40}$  ( $\bullet$ , periclase: JCPDS file no. 82–1316) and unknown phase ( $\circ$ ) were formed. The occurring of  $Bi_{23}(Bi_{1.04}Fe_{0.84})O_{40}$  phase indicates that the chemical reaction between  $Bi_2O_3$  and  $Fe_2O_3$  during the BF formation process as seen the XRD patterns of (1-x)BF-xPMN where x=0.0 (Fig. 1 (a)), For unknown phase, it could not be matched with related JCPDS files. More interestingly, at a higher sintering temperature (900 °C), the reaction between BF and PMN phases was occurred and produced the secondary phase more than using a lower temperature (800 °C) because the energy is high enough to activate the reaction of PMN.

Backscattered electron (BSE) images of BF-PMN multiferroic composites sintered at different temperatures are compared in Figs. 3 and 4. The BSE pictures of these composites from sintering temperature at 800 °C demonstrate that the grain size of BF and PMN are found to be significantly different and pointed out a heterogeneous microstructure. Especially, from Figs. 3 (a)–(c), it can be noted that the microstructure consists of small grains of about 0.7  $\mu$ m and abnormally growth grains of about 6.5–13  $\mu$ m. The abnormal grain growth may be related to the mass transfer during grain growth [22]. In addition to the BF matrix phase, two secondary phases were identified by X–ray diffraction in PMN–added samples, Bi<sub>24</sub>(Bi<sub>1.04</sub>Fe<sub>0.84</sub>)O<sub>40</sub> and unknown phases in BF-PMN with x = 10–30 wt%. EDS analysis for the sample of x = 20 wt% showed that the irregular growth grains, lighted regions, were rich in Bi with small amounts of Fe. These grains are probably the

Bi<sub>24</sub>(Bi<sub>1.04</sub>Fe<sub>0.84</sub>)O<sub>40</sub> phase identified by X-ray diffraction. On the other hand, the dark colored, more uniform grains were rich in Fe which is probably the unknown phase, Moreover, EDS analysis for x = 40 wt% sample showed that the dark phase contained primarily Bi, Fe and small amounts of Mg. The light-colored phase contained more amounts of Mg, Nb, Pb and small amount of Bi and Fe, which indicated that the BF phase was mainly in the dark regions and the PMN phase was mainly in the light-colored regions and interdiffusion occurred between the two phases during firing. The BSE microstructure of samples prepared with 10 and 20 wt% PMN and sintered at 900 °C were very similar to those shown in Figs. 4 (a) and (b).

When PMN was added with 40 and 50 wt%, then there were major changes to the microstructure for both sintering conditions as shown in Figs. 3 (d), (e) and 4 (c)–(e). Moreover, the micrographs demonstrate that these composites possess high density and well–defined grains. The grains of BF and PMN are distributed homogeneously. We cannot catch what role the BF plays in influencing the grain growth; however, one can takes note of that not only the grain size but also the grain morphology was changed. The changed in grain size seems to be finished by disintegration of big grains into small ones, as seen from Figs. 3 and 4. Moreover, the average grain size of BF and PMN was increased with increasing sintering temperature.

Figs. 5 and 6 show the temperature dependence of the real part of the dielectric constant (\$\varepsilon\$) for (1-x)BF-xPMN composites. The room temperature dielectric constant values at 10 kHz-1 MHz frequencies are given in Table 1. The dielectric constant seems to relate to the effect of firing temperature on density of the final products. A very abnormal diffuse dielectric patterns, containing high dielectric constant peak (on the order of 10<sup>3</sup>), is observed in the \$\varepsilon\$-T curve around 330 °C at 10 kHz during the heating process. However, the dielectric

constant for all composites appears to be lower and also boarder than for pure BF ceramics. In addition, since PMN has a pseudo-cubic symmetry at temperature above -10 °C, it may reduce the dielectric constant values. There are various reasons to explain the dielectric response of composite materials. Ausloo [23] reported the board dielectric constant curve of the results of clustering effect including the shape of the cluster and heterogeneity effect.

The maximum of dielectric constant shifts toward higher sintering temperature, moreover, it can be noticed that these composites exhibit two dielectric anomalies. First, anomaly occurs near 230 °C, which seems to agree with the dielectric measurements in literatures [24–26]. While the other anomaly appears near the magnetic transition temperature of the ferrite BF phases (around 330 °C). This anomaly corresponds to the antiferromagnetic to paramagnetic phase transition at Néel temperature.

The room temperature magnetic properties of the (1-x)BF-xPMN composites sintered at 800 and 900 °C is shown in Figs. 7 and 8, respectively, at field of less than 8 kOe. The M-H hysteresis loops show interesting features. These composite exhibit typical magnetic hysteresis loops of the magnetic materials, indicating that the composites are magnetically ordered materials. In all samples, saturation has been achieved by 7.5 kOe, with values in the range 1–5.5 emu/g. Values of the remanent magnetization  $(M_T)$  for x=10 wt% is 0.30 (0.50 and for x=20, 30, 40 and 50 wt%, the values of 0.56 (0.65), 0.82 (0.93), 0.55 (1.13) and 0.27 (0.73) emu/g were obtained, respectively, when samples were sintered at 800 and 900 °C as displaced in Table 2. It can be seen that samples sintered at 800 °C prepared with higher contents of PMN addition (40 and 50 wt% of PMN) show corresponding lower level of  $M_T$ . Decrease in  $M_T$  may be attributed to the influence of the pinning effect of the non–magnetic phase PMN, as also reported in BF/PT and PT/NiFe<sub>2</sub>O<sub>4</sub> composites [10, 27]. For composites with x=0.1–0.3, a large induced magnetization is observed than that of pure BF ceramic,

with the same result in BF/BT system [28]. Moreover, the coercivity ( $H_c$ ) values of all the composites are in the range of 0.036–0.041 kOe. The increase of  $H_c$  with an increase in PMN contents shows that the magnetization is weak. This is due to the presence of non–magnetic phase, in which domain wall pinning can occur, around magnetic phase as shown in Figs. 3 and 4.

#### 4. Conclusions

This preliminary study shows that biphasic multiferroic composites consisting of ferrite BF and relaxor ferroelectric PMN can be successfully prepared. The coexistence of BF and PMN phases in these composites has been confirmed from XRD analysis and SEM images. Dielectric constant increase with increasing sintering temperature and PMN phase has no significantly effect on dielectric constant values. All the composites reveal magnetic hysteresis loops, showing soft magnetic nature, and the saturation magnetization values are found to increase with increasing PMN contents up to 30 wt%.

#### Acknowledgements

We thank the Thailand Research Fund (TRF) and Faculty of Science of Maejo University for financial supports. Also acknowledged for additional support is Processing Technology of Materials Research Laboratory (PTMRL) for all the technical support.

#### References

 E.K.H. Salje, Phase Transitions in Ferroelastic and co–Elastic Crystals, Cambridge Univ. Press, Cambridge, 1990.

- 2. G.A. Smolenskii, I. Chupis, Sov. Phys. Usp. 25 (1982) 475-493.
- 3. F. Kubel, H. Schimid, Acta Crystallogr. B 46 (1990) 698-702.
- C. Ederer, N.A. Spaldin, Phys. Rev. B 71 (2005) 060401–060404.
- 5. D. Ricinschi, K.Y. Yun, M. Okuyama, J. Phys.: Condens. Matter. 18 (2006) L97-L105.
- 6. K. No, M.F. Berard, J. Solid State Chem. 90 (1991) 126-146.
- A. Hanumaiah, T. Bhimasankaram, S.V. Suryanarayana, G.S. Kumar, Bull. Mater. Sci. 17 (1994) 405–409.
- C. Ang, Z. Yu, B. Yahua, D. Xi, J. Qin, J. Phys.: Condens. Matter. 9 (1994) 3553– 3558.
- Landolt-Börnstein, Numerial Data and Functional Relationships in Science and Technology, New Series Group III, Springer-Verlag, Berlin, 1969.
- R.S. Tebble, D.J. Craik, Magnetic Materials, Chapter 7, Wiley-Interscience, London, 1969.
- R. Mazunder, P. Sujatha Devi, D. Blaattacharya, P. Choudhury, A. Sen, Appl. Phys. Lett. 91 (2007) 062510–062513.
- A.J. Moulson, J.M. Herbert, Electroceramics, second ed., John Wiley & Sons, Chichester, 2003.
- 13. G.H. Haertling, J. Am. Ceram. Soc. 82 (1999) 797-818.
- R. Wongmaneerung, P. Jantaratana, R. Yimnirun, S. Ananta, J. Supercond. Nov. Magn. (2012) DOI 10.1007/s10948-012-1733-8.
- D.R. Patil, S.S. Chougule, S.A. Lokare, B.K. Chougule, J. Alloys Compd. 452 (2008) 414–418.
- D.R. Patil, B.K. Chougule, J. Alloys Compd. 458 (2008) 335–339.
- 17. D.R. Patil, S.A. Lokare, S.S. Chougule, B.K. Chougule, Physica B 400 (2007) 77-82.

- G.A. Smolenskii, A.I. Agranovskaya, Sov. Phys. Tech. Phys., (Engl. Tranl.) 3 (1958)
   1380–1382.
- 19. L.E. Cross, S.J. Jang, R.E. Newnham, K. Uchino, Ferroelectrics 23 (1980) 187-191.
- R. Wongmaneerung, R. Yimnirun, S. Ananta, J. Alloys Compd. 477 (2009) 805–810.
- F. Prihor, P. Postolache, L. Curecheriu, A. Ianculescu, L. Mitoseriu, Ferroelectrics 391 (2009) 76–82.
- 22. Z. Yue, S. Chen, X. Qi, Z. Gui, L. Li, J. Alloys Compd. 375 (2004) 243-248.
- 23. M. Ausloos, J. Phys. C Solid State Phys. 18 (1985) L1163-L1168.
- 24. W.M. Zhu, Z.-G. Ye, Ceram. Int. 30 (2004) 1435-1442.
- N.N. Krainik, N.P. Khuchua, V.V. Zhanova, V.A. Evseev, Sov. Phys. Solid State 8 (1966) 654-658.
- D.-C. Jia, J.-H. Xu, H. Ke, W. Wang, Y. Zhou, J. Eur. Ceram. Soc. 29 (2009) 3099– 3103.
- L. Zhu, Y. Dong, X. Zhang, Y. Yao, W. Weng, G. Han, N. Ma, P. Du, J. Alloys Compd. 503 (2010) 426–430.
- 28. N. Itoh, T. Shimura, W. Sakamoto, T. Yogo, Ferroelectrics 356 (2007) 19-23.

#### List of Table Captions

Table 1 Dielectric properties of (1-x)BF-xPMN multiferroic composites.

Table 2 Variation of ramanent magnetization and coercivity of (1-x)BF-xPMN multiferroic composites.

#### List of Figure Captions

Fig. 1 XRD patterns of (1-x)BF-xPMN multiferroic composites sintered at 800 °C with (a) 0, (b) 10, (c) 20, (d) 30, (e) 40, (f) 50 and (g) 100 wt% of PMN.

Fig. 2 XRD patterns of (1-x)BF-xPMN multiferroic composites sintered at 900 °C with (a) 0, (b) 10, (c) 20, (d) 30, (e) 40, (f) 50 and (g) 100 wt% of PMN.

Fig. 3 SEM micrographs of (1-x)BF-xPMN multiferroic composites sintered at 800 °C with (a) 10, (b) 20, (c) 30, (d) 40 and (e) 50 wt% of PMN.

Fig. 4 SEM micrographs of (1-x)BF-xPMN multiferroic composites sintered at 900 °C with (a) 10, (b) 20, (c) 30, (d) 40 and (e) 50 wt% of PMN.

Fig. 5 Temperature dependence of the real part of dielectric constant for (1-x)BF-xPMN multiferroic composites sintered at 800 °C with (a) 10, (b) 20 and (c) 30 wt% of PMN.

Fig. 6 Temperature dependence of the real part of dielectric constant for (1-x)BF-xPMN multiferroic composites sintered at 900 °C with (a) 10, (b) 20 and (c) 30 wt% of PMN.

Fig. 7 M–H hysteresis loops of (1-x)BF–xPMN multiferroic composites measured at room temperature: sintered at 800  $^{\circ}C$ .

Fig. 8 M–H hysteresis loops of (1–x)BF–xPMN multiferroic composites measured at room temperature: sintered at 900  $^{\circ}$ C.

Table 1				
Sintering	Composition (x)	Frequency	$T_{\rm N}$	Er at T
(°C for 2 h)	(weight fraction)	(kHz)	(°C)	
800	0.1	10	300	1398
		100	300	727
		1000	320	352
	0.2	10	440	3940
		100	380	1508
		1000	380	816
	0.3	10	360	1190
		100	360	676
		1000	360	350
900	0.1	10	270	6675
		100	280	3190
		1000	280	1013
	0.2	10	320	2600
		100	320	1146
		1000	320	550
	0.3	10	270	1092

Table 2

Sintering temperature (°C for 2 h)	Composition (x) (weight fraction)	M <sub>S</sub> (emu/g)	M <sub>r</sub> (emu/g)	H <sub>C</sub> (Oe)
0.2	2.60	0.56	37.02	
0.3	4.17	0.82	36.76	
0.4	2.55	0.55	37.01	
0.5	1.32	0.27	36.98	
900	0.1	2.13	0.50	40.71
	0.2	3.11	0.65	40.40
	0.3	4.70	0.93	40.72
	0.4	5.25	1.13	40.71
	0.5	3.19	0.73	40.73

### Figure(s)

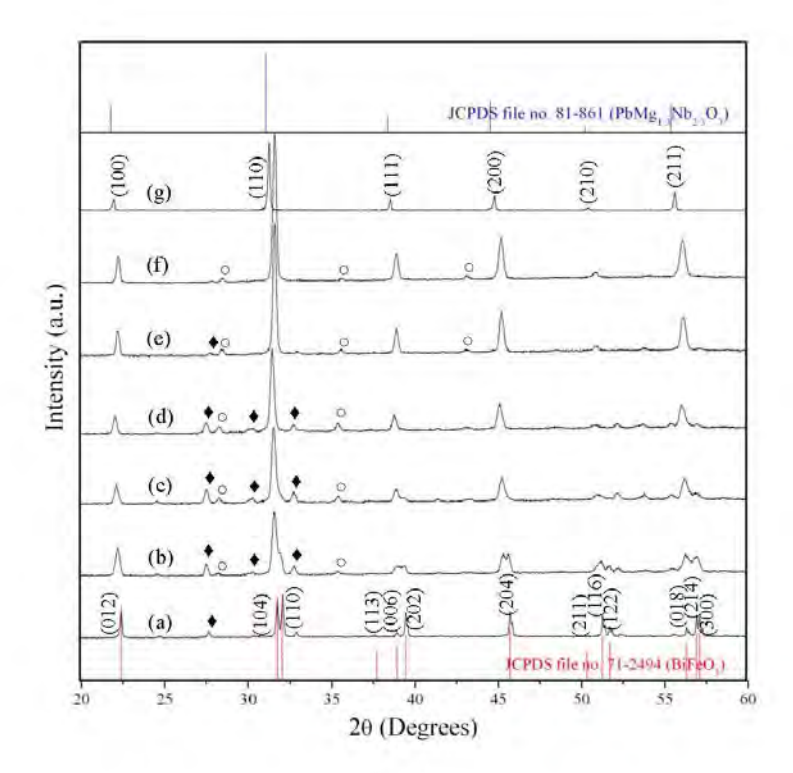


Fig. 1

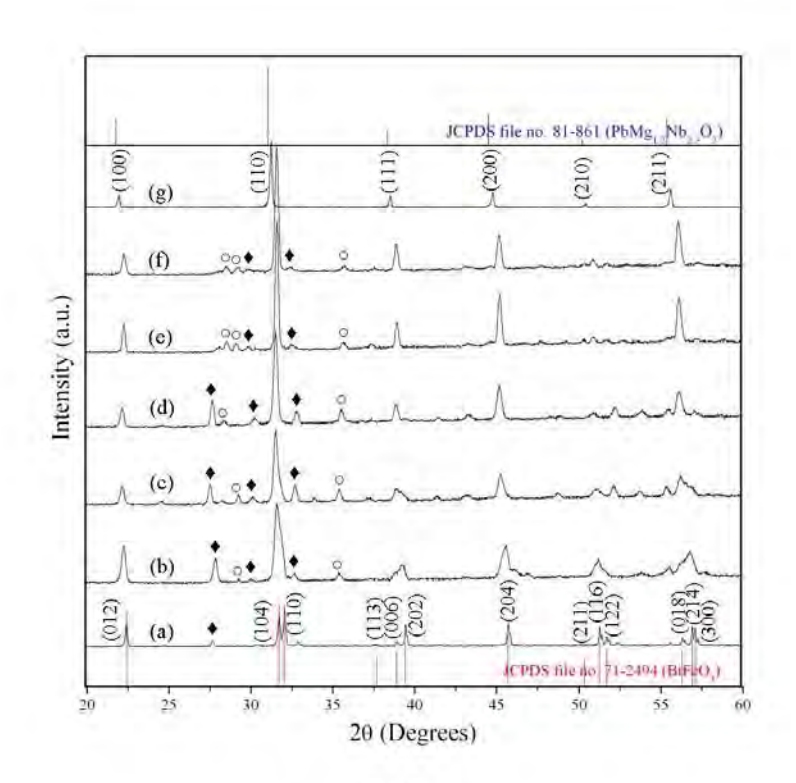


Fig. 2

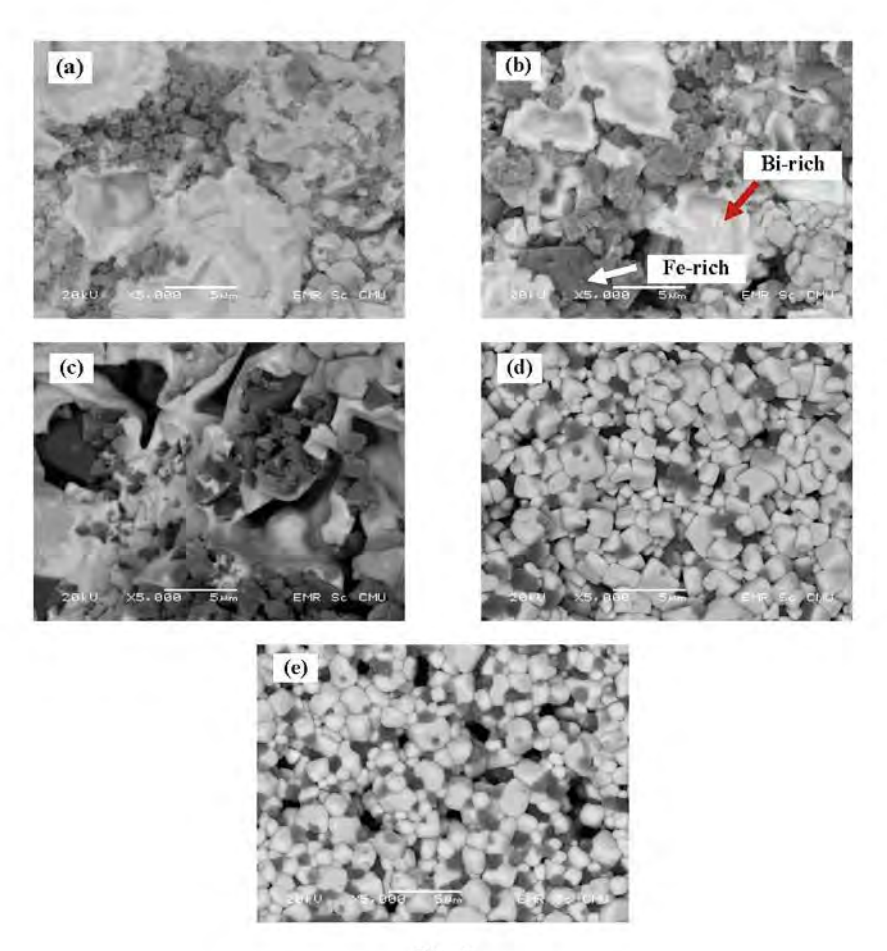


Fig. 3

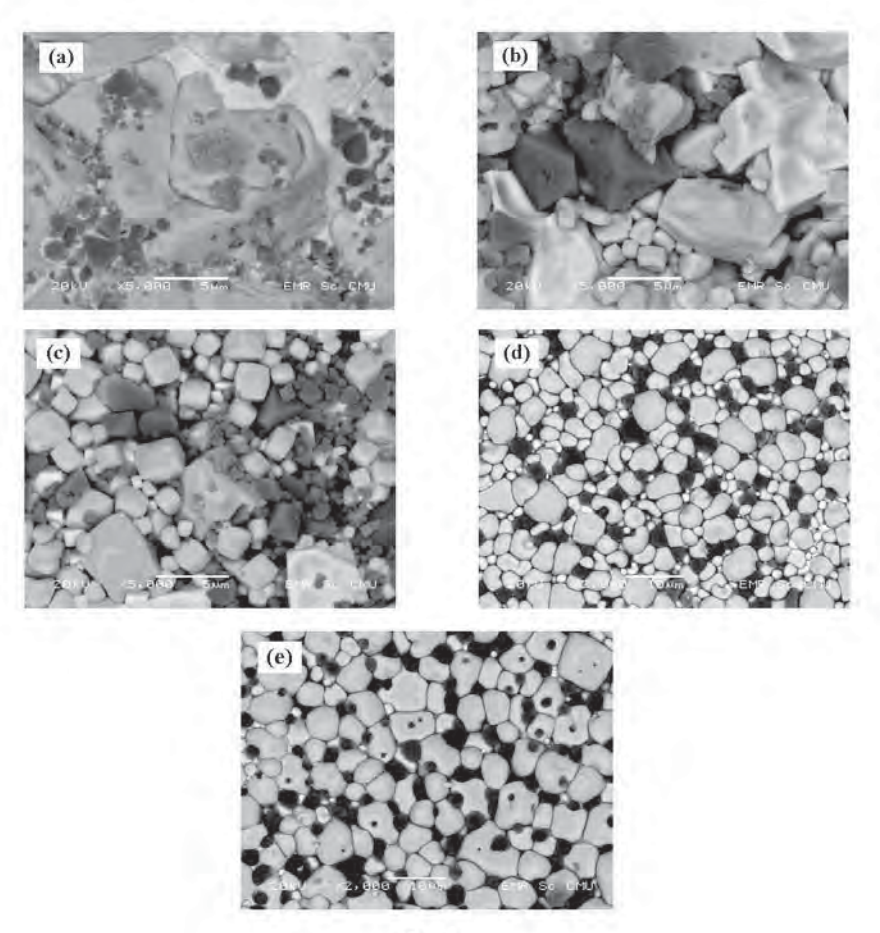


Fig. 4

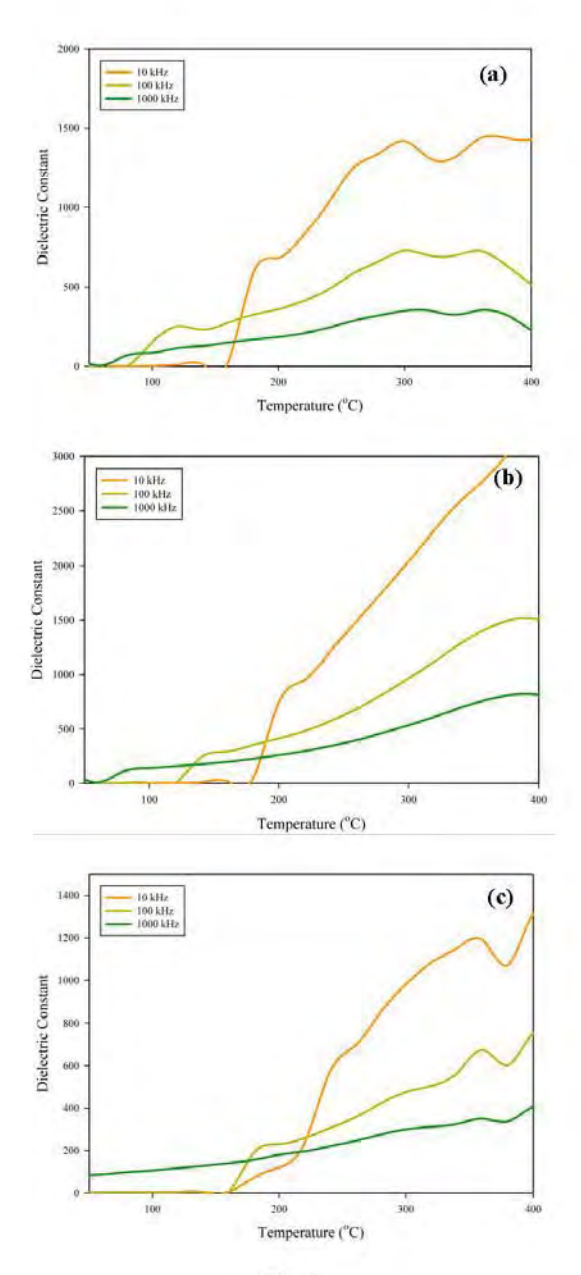


Fig. 5

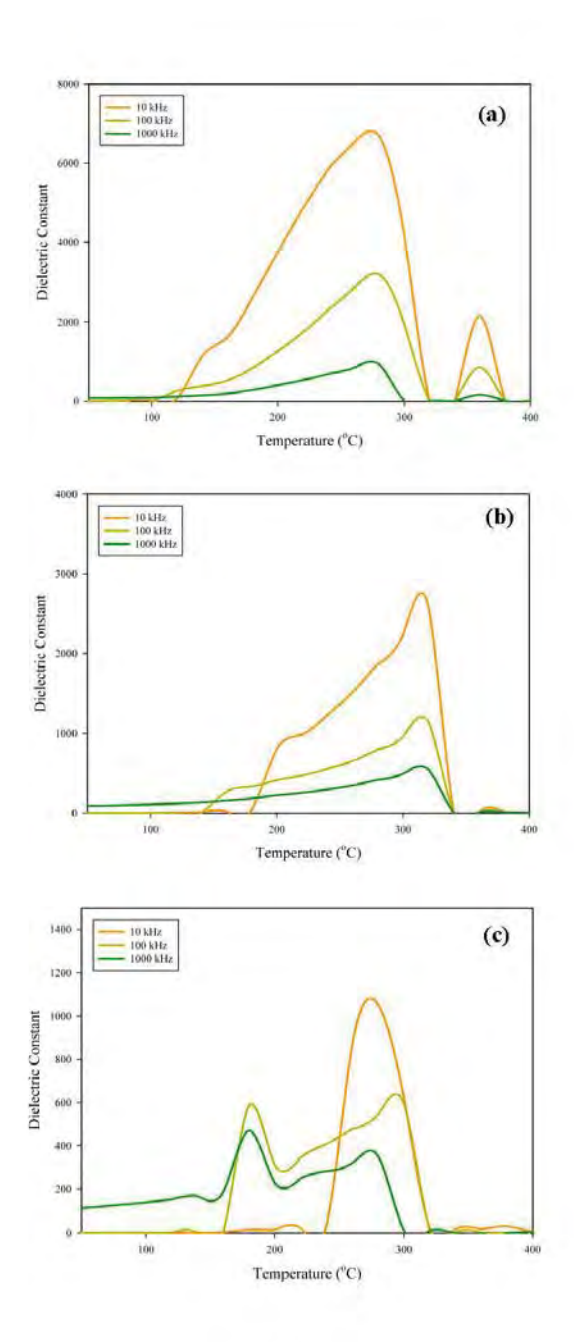


Fig. 6

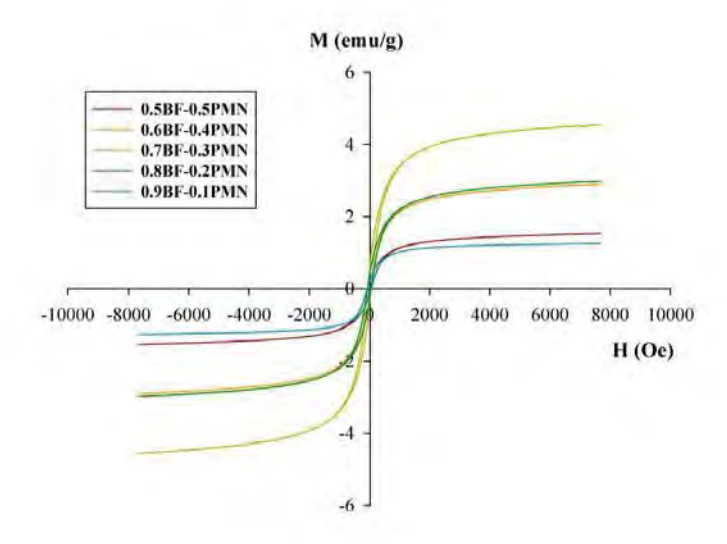


Fig. 7

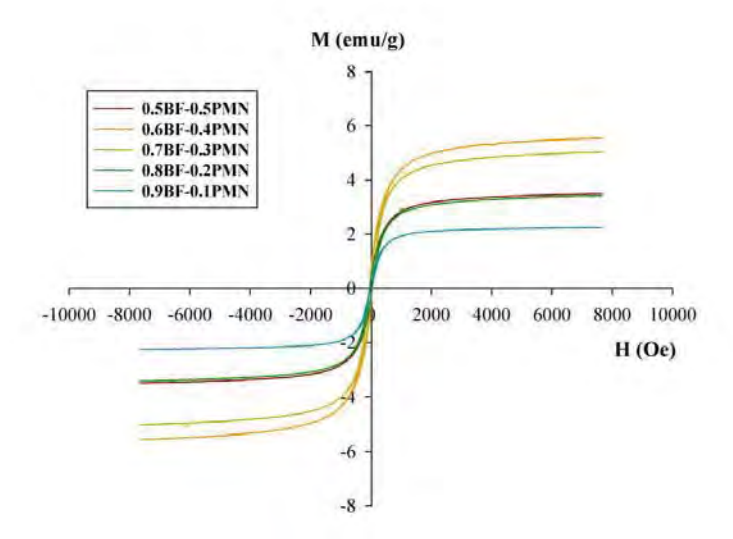


Fig. 8

Manuscript ที่ได้จัดส่งวารสาร Journal of Superconductivity and Novel Magmetism

Phase formation, Microstructure and Magnetic Properties of (1-x)BiFeO<sub>3</sub>-

 $x(0.9Pb(Mg_{1/3}Nb_{2/3})O_3-0.1PbTiO_3)$ 

Rewadee Wongmaneerung<sup>1\*</sup>, Pongsakorn Jantaratana<sup>2</sup>, Rattikorn Yimnirun<sup>3</sup>

and Supon Ananta<sup>4</sup>

<sup>1</sup>Faculty of Science, Maejo University, Chiang Mai 50290, Thailand

<sup>2</sup>Department of Physics, Kasetsart University, Bangkok 10900, Thailand

<sup>3</sup>School of Physics, Institute of Science, Suranaree University of Technology,

Nakhon Ratchasima 30000, Thailand

<sup>4</sup>Department of Physics and Materials Science, Faculty of Science, Chiang Mai University,

Chiang Mai 50200, Thailand

Abstract

Multiferroic composites containing bismuth ferrite (BF) and lead magnesium

niobate-lead titanate (0.9PMN-0.1PT) phases were fabricated by solid-state reaction, with

10-50 % wt of 0.9PMN-0.1PT. The phase formation and microstructure were investigated

by X-ray diffraction (XRD) and scanning electron microscope (SEM). Vibrating sample

magnetometer (VSM) was used to characterize the magnetic properties. The results

indicate that all composites show the perovskite structure and PMN-PT phase is

compatible with BF phase. The microstructure display the mix phases between BF, PMN

and PT phases. Moreover, the composites exhibited typical magnetic hysteresis (M-H)

Corresponding author: Tel.: 66 53 873515 Fax: 66 53 878225

loops at room temperature. The maximum saturation magnetization  $M_S$  is observed for x =

30 and 40 wt% and then decreases with PMN-PT contents is less than 10 wt%.

*Keywords:* Multiferroic; Composites; BiFeO<sub>3</sub>-based ceramics; Magnetic Properties

1. Introduction

Perovskite solid-solutions have been an active area of research due to their

importance in ferroelectric, ferromagnetic and piezoelectric applications along with their

fascinating physical properties [1–3]. In particular, Bi–based ferroelectric are under intense

investigation, because of its multiferroic properties i.e., ferroelectricity with high Curie

temperature  $(T_{\rm C})$  [4] and antiferromagnetic properties below Néel temperature  $(T_{\rm N})$  [5].

However, the choice of single-phase materials exhibiting coexistence of strong ferro-

ferrimagnetism and ferroelectricity is limited. Therefore, the composite concept has been

proposed.

The emergence of new class of two-phase materials, namely, multiferroic

composites/ferroelectric-ferromagnetic or dielectric-ferromagnetic composites have been

attracted widely attentions from academics and industries because composites are desirable

for the synthesis of materials with unique or improved properties. The sum properties of

the composites such as dielectric properties, ferroelectric properties, electrical

conductivity, ferromagnetic properties, density, etc., are also equally important as they

affect the product property and hence its application in various practical devices.

Multiferroic BiFeO<sub>3</sub> (BF) shows antiferromagnetic G-type spin configuration

along the [111]<sub>c</sub> or [111]<sub>h</sub> directions in its pseudocubic or rhombohedral structure.

Interestingly, this ferromagnetic BF exhibits characteristic features in dielectric properties

105

around the magnetic transition temperature, highlighting useful multiferroic behavior [6]. Moreover, BF compound is one of the ferro–electromagnetic multiferroic in which ferroelectric ( $T_{\rm C}=830~{\rm ^{\circ}C}$ ) and antiferromagnetic ( $T_{\rm N}=370~{\rm ^{\circ}C}$ ) [4,7] order parameter co–exist up to quite high temperature. One of the main obstacles for BF applications is large leakage current. Recently, for high temperature applications and solve the problems, the binary system of multiferroic composite has been widely studies [8–10]. In this research report, an attempt has been made to study the ternary system BiFeO<sub>3</sub>–Pb(Mg<sub>1/3</sub>Nb<sub>2/3</sub>)O<sub>3</sub>–PbTiO<sub>3</sub> aiming at the development of multiferroic materials with desirable magnetic properties with reduction in leakage current. PbTiO<sub>3</sub> (PT) was employed to form multiferroic composites with BF to improve the electro–magnetic properties because of its high ferroelectric transition temperature, large polarization and strong ability to stability the perovskite phase [11,12]. On the other hand, Pb(Mg<sub>1/3</sub>Nb<sub>2/3</sub>)O<sub>3</sub> (PMN) has not been use for multiferroic composites.

#### 2. Experimental

The (1-x)BF-x(0.9PMN-0.1PT) (where x = 10, 20, 30, 40 and 50 %wt) composite materials were prepared by standard ceramic method. Firstly, laboratory grade reagents of  $Bi_2O_3$  and  $Fe_2O_3$  were used to prepare the  $BiFeO_3$  ferrite phase. The  $Pb(Mg_{1/3}Nb_{2/3})O_3$  and  $PbTiO_3$  ferroelectric phases were synthesized from high purity oxides of PbO, MgO,  $Nb_2O_5$  and  $TiO_2$  powders. BF, PMN and PT powders were prepared separately. The constituent BF compounds in suitable stoichiometry were thoroughly mixed in a ball milling for 24 h while PMN and PT phases were milled by vibro-milling for 1 h. The ferrite and ferroelectric phase were calcined separately at 850, 950 and 600 °C for 2 h, respectively. Multiferroic composites of (1-x)BF-x(0.9PMN-0.1PT) were prepared by

milling in a ball-mill for 24 h. The composite powders were pressed into disc pellets of 10 mm in diameter and 1.5 mm in thickness using a uniaxial pressing. The pellets were sintered at 800 and 900 °C for 2 h in air.

The X-ray diffraction patterns of the composites were recorded by X-ray powder diffractometer with Cu  $K_{\alpha}$  radiation at room temperature. The microstructure of composites was examined with a Field Emission Scanning Electron Microscope (FE–SEM) in backscattering electron mode. The magnetic data was recorded with the help of vibrating sample magnetometer (VSM) by applying an external magnetic field of 8 kOe at room temperature.

#### 3. Results and discussion

The typical X-ray diffraction patterns of (1-x)BF-x(0.9PMN-0.1PT) multiferroic composites with sintering temperature at 800 and 900 °C are shown in Figs. 1 and 2, respectively. It is clearly seen that ferrite and ferroelectric phases are indentified in composites. No phases other than BF-PMN-PT were observed in the X-ray analysis. It suggests that no significant chemical reaction were taken place during firing. All the reflection peaks were indexed using observed inter-plane spacing (d) were determined. The observed d values of all diffraction lines of (1-x)BF-x(0.9PMN-0.1PT) composites with different x content suggest that there is a change in the crystal structure from rhombohedral to mix cubic-tetragonal. A comparison between the XRD patterns reveals that the intensity of 0.9PMN-0.1PT peaks increase with increasing percentage of PMN-PT in these composites, while the intensity of ferrite peaks reduce continuously. As shown in the Figs. 1(b) and 2(b), the most strong diffraction peaks (104)(110) of BF shift toward lower angles for the composites. Especially, for Fig. 2, it can be easily seen that splitting

peaks (006)(200) shift toward lower angles and become one diffraction peak (111). It may be explained by the fact that the radius of Pb<sup>2+</sup> (119 pm) is larger than that of Bi<sup>3+</sup> (103 pm) and Mg<sup>2+</sup> (72 pm), Nb<sup>5+</sup> (64 pm) and Ti<sup>4+</sup> (61 pm) are larger than that of or Fe<sup>3+</sup> (49 pm) [13], resulting in an increase of unit cell volume with a shift of diffraction peaks toward lower angles.

The backscattered electron images of composite samples with various compositions are shown in Figs. 3 and 4 (sintered at 800 and 900 °C, respectively). Since the composites are multiphase, it is desirable to know the distribution of the constituent phases which are observed in the microstructure. It should be noted that the overall microstructure of composites sintered at 800 and 900 °C are totally different from those observed in the BFbased solid-solution case [14,15]. As a result, the microstructure became non-uniform. However, the uniform structure were obtained at x = 30 %wt for both sintering temperature. In the images, the dark color grains are ferrite grains and the light color ones are PMN-PT ferroelectric grains. It is very clear that two component phases are co-existed in the sintered composites. It is also identified that the grain sizes of two phases vary with the relative content of the components. Moreover, the grain size of PMN-PT and BF are found to be different. The ferrite grains are found to be of 0.5-1.25 µm size while for PMN-PT grain size varies in the range of 1.0-3.75 µm. The average grain size of ferroelectric phase is found larger than the ferrite phase in these composites. However, there were some large pores and agglomeration of the ferrite particles. Those could be found in the composites containing 10 and 20 % wt of PMN-PT.

The SEM results substantiate with XRD results, indicating the successful formation of BF-PMN-PT composites. The microstructures of composites did not show any third phase caused by chemical reaction between BF and PMN-PT phases. For higher-temperature sintering, a pronounced second phase is segregated at the grain boundaries.

The observation of these layers could be attributed to a liquid–phase formation during the sintering process as proposed by many researchers [16,17]. Uneven grain boundaries were also observed in Fig. 4(a) and (e). This uneven grain boundary seems to be a diffusion induced grain boundary migration [18]. In general, this mechanism is the evidence of the chemical composition gradient. Therefore, dissolution of Fe<sup>3+</sup> ions from ferrite into ferroelectric phase can be expected in this composition. In this work, we did not control the connectivity, the actual connectivity was random mixture of 3–0 and 0–3 connectivities [19].

The magnetic hysteresis (M–H) loops of BF–PMN–PT composites are investigated at room temperature using VSM with an applied magnetic field of -8 kOe  $\leq H \leq$  8 kOe as shown in Figs. 5 and 6 which samples sintered at 800 and 900 °C, respectively. The magnetic properties of materials are usually characterized by a hysteresis loop, which gives the behavior of materials when excited by an external magnetic field. Moreover, the magnetic characteristics of the composites follow from the ferrite's properties, which are sensitive to composition, processing and firing conditions. If the presence of the ferroelectric in these composites does not change the intrinsic magnetic properties of the BF phase, a proportional reduction of the sum magnetization of composites with reducing the amount of the ferrite phase is expected. From the graphs, it is noted that composites exhibits a typical magnetic hysteresis, indicating that the composites in the BF-PMN-PT system are magnetically ordered. For x = 10, the saturation magnetization is 2.45 (1.46) emu/g, and for x = 20, 30, 40 and 50, the values of 2.10 (2.82), 0.97 (4.67), 3.28 (3.86) and 1.26 (2.84) emu/g were obtained, respectively, when samples were sintered at 800 °C (900 °C). These values are larger than the value of ~0.2 emu/g for pure BF [11]. The saturation magnetization  $(M_S)$  of the composites decreases with an increase in "x" as shown in Figs. 7 and 8. Figs. 7 and 8 show the composition dependence of the saturation magnetization for the samples sintered at 800 and 900 °C, respectively.

From Fig. 7, when the amount of PMN–PT increases, the dilution effect dominates the magnetic properties of composites. This behavior can be attributed to size effect with two contributing factors: the structural distortion in the perovskite i.e., the content spin arrangement of unpaired electron on Fe<sup>3+</sup> ions is caused by incorporating Pb<sup>2+</sup> ions to A sites and/or Mg<sup>2+</sup>, Nb<sup>5+</sup> and Ti<sup>4+</sup> ions to B sites of the perovskite structure of BF [20] and at low ferrite concentration, the ferrite crystallite size is smaller. Other possible reason is the individual ferrite grains acts as center of magnetization and ferroelectric materials incorporate into the ferrite phase and break the magnetic circuit [21]. This results in decrease of magnetic parameters with increasing PMN–PT concentration in multiferroic composites.

#### 4. Conclusion

Composite materials consisting BiFeO<sub>3</sub> ferrite as phase and 0.9Pb(Mg<sub>1/3</sub>Nb<sub>2/3</sub>)O<sub>3</sub>-0.1PbTiO<sub>3</sub> as a ferroelectric phase have been synthesized successfully by using solid-state reaction method. The coexistence of BF and PMN-PT phases in these composites has been confirmed from the XRD analysis and SEM images. The sintered composites were consisted of BiFeO<sub>3</sub> and 0.9Pb(Mg<sub>1/3</sub>Nb<sub>2/3</sub>)O<sub>3</sub>–0.1PbTiO<sub>3</sub> phases and no impurity phase was detected by XRD spectra. The SEM observations revealed that the co-existed two phases affect the sintering behavior and grain growth of components. These composites show typical magnetic behavior, which found to exhibit good magnetic properties. Moreover, the saturation magnetization values are found to decrease with increasing PMN-PT content.

#### Acknowledgements

The authors would like to thank the Thailand Research Fund (TRF) and the Faculties of Science of Maejo University for their financial support.

#### References

- 1. Cohen, R.E.: Nature **358**, 136 (1992).
- 2. Bellaiche, L., Garcia, A., Vanderbilt, D.: Phys. Rev. Lett. **84**, 5427 (2005).
- 3. Grinberg, I., Cooper, V.R., Rappe, A.M.: Nature 419, 909 (2002).
- 4. Smolenskii, G.A., Isupov, V., Agranovskaya, A., Krainik, N.: Sov. Phys.–Solid State 2, 2651 (1961).
- Smolenskii, G.A., Yudin, V.M., Sher, E.S., Stolypin, Y.E.: Sov. Phys.–JEPT 16, 622 (1963).
- 6. Mazumder, R., Sujatha Devi, P., Bhattacharya, D., Choudhury, P., Sen, A.: Appl. Phys. Lett. **91**, 06251 (2007) 0.
- 7. Venevtsev, Yu. N., Zhdanov, G., Sdovev, S.: Sov. Phys. Crystallogr. 4, 538 (1960).
- 8. Zhoua, Y., Zhang, J., Li, L., Su, Y., Cheng, J., Cao, S.: J. Alloy. Compd. **484**, 535 (2009).
- 9. Narendra Babu, S., Srinivas, K., Bhimasankaram, T.: J. Magn. Magn. Mater. **321**, 3764 (2009).
- 10. Corral-Flores, V., Bueno-Baqués, D., Ziolo, R.F.: Acta Mater. 58, 764 (2010).

- 11. Singh, K., Negi, N.S., Kotnala, R.K., Singh, M.: Solid State Commun. **148**, 18 (2008).
- 12. Zhu, W.M., Ye, Z.-G.: Ceram. Int. **30**, 1435 (2004).
- 13. Shannon, R.D.: Acta Crystallogr. A 32, 751 (1974).
- 14. Mahesh Kumar, M., Srinath, S., Kumar, G.S., Suryanarayana, S.V.: J. Magn. Magn. Mater. 188, 203 (1998).
- PrihorGheorghiu, F., Ianculescu, A., Postolache, P., Lupu, N., Dobromir, M., Luca,
   D., Mitoseriu, L.: J. Alloy. Compd. 506, 862 (2010).
- 16. Wang, H.C., Schulze, W.A.: J. Am. Ceram. Soc. 73, 825 (1990).
- 17. Gupta, S.M., Kulkarni, A.R.: J. Mater. Res. 10, 953 (1995).
- 18. Park, J.K., Kim, D.Y.: J. Am. Ceram. Soc. 79, 1405 (1996).
- 19. Newnham, R.E.: Ferroelectrics **68**, 1 (1986).
- 20. Rai, R., Kholkin, A.L., Sharma, S.: J. Alloy. Compd. **506**, 815 (2010).
- 21. Kanamadi, C.M., Das, B.K., Kim, C.W., Kang, D.I., Cha, H.G., Ji, E.S., Jadhav, A.P., Jun, B.–E., Jeong, J.H., Choi, B.C., Chougule, B.K., Kang, Y.S.: Mater. Chem. Phys. 116, 6 (2009).

### **List of Table Captions**

Table 1 Magnetic properties of (1-x)BF-x(0.9PMN-0.1PT) multiferroic composites

#### **List of Figure Captions**

Fig. 1 XRD patterns of (1-x)BF-x(0.9PMN-0.1PT) multiferroic composites sintered at 800 °C with (a) 10, (b) 20, (c) 30, (d) 40 and (e) 50 % wt of 0.9PMN-0.1PT.

Fig. 2 XRD patterns of (1-x)BF-x(0.9PMN-0.1PT) multiferroic composites sintered at 900 °C with (a) 10, (b) 20, (c) 30, (d) 40 and (e) 50 % wt of 0.9PMN-0.1PT.

Fig. 3 SEM micrographs of (1-x)BF-x(0.9PMN-0.1PT) multiferroic composites sintered at 800 °C with (a) 10, (b) 20, (c) 30, (d) 40 and (e) 50 %wt of 0.9PMN-0.1PT.

Fig. 4 SEM micrographs of (1-x)BF-x(0.9PMN-0.1PT) multiferroic composites sintered at 900 °C with (a) 10, (b) 20, (c) 30, (d) 40 and (e) 50 % wt of 0.9PMN-0.1PT.

Fig. 5 M–H hysteresis loops of (1-x)BF–x(0.9PMN–0.1PT) multiferroic composites sintered at 800  $^{\circ}C$ .

Fig. 6 M–H hysteresis loops of (1-x)BF–x(0.9PMN–0.1PT) multiferroic composites sintered at 900  $^{\circ}C$ .

Fig. 7 Composition dependence of the  $M_{\rm S}$  and  $H_{\rm C}$  of  $(1-x){\rm BF}-x(0.9{\rm PMN}-0.1{\rm PT})$  multiferroic composites sintered at 800 °C.

Fig. 8 Composition dependence of the  $M_{\rm S}$  and  $H_{\rm C}$  of  $(1-x){\rm BF}-x(0.9{\rm PMN}-0.1{\rm PT})$  multiferroic composites sintered at 900 °C.

Table 1

Sintering temperature (°C for 2 h)	Composition (x)  (weight  fraction)	Magnetic properties		
		Ms (	<i>M</i> r	Нс
		(emu/g)	(emu/g)	(Oe)
800	10	2.45	0.39	55.36
	20	2.10	0.30	62.90
	30	0.97	0.17	72.97
	40	3.28	0.62	50.33
	50	1.26	0.19	60.39
900	10	1.46	0.18	47.81
	20	2.82	0.39	55.36
	30	4.67	0.57	42.78
	40	3.86	0.51	52.84
	50	2.84	0.33	40.26

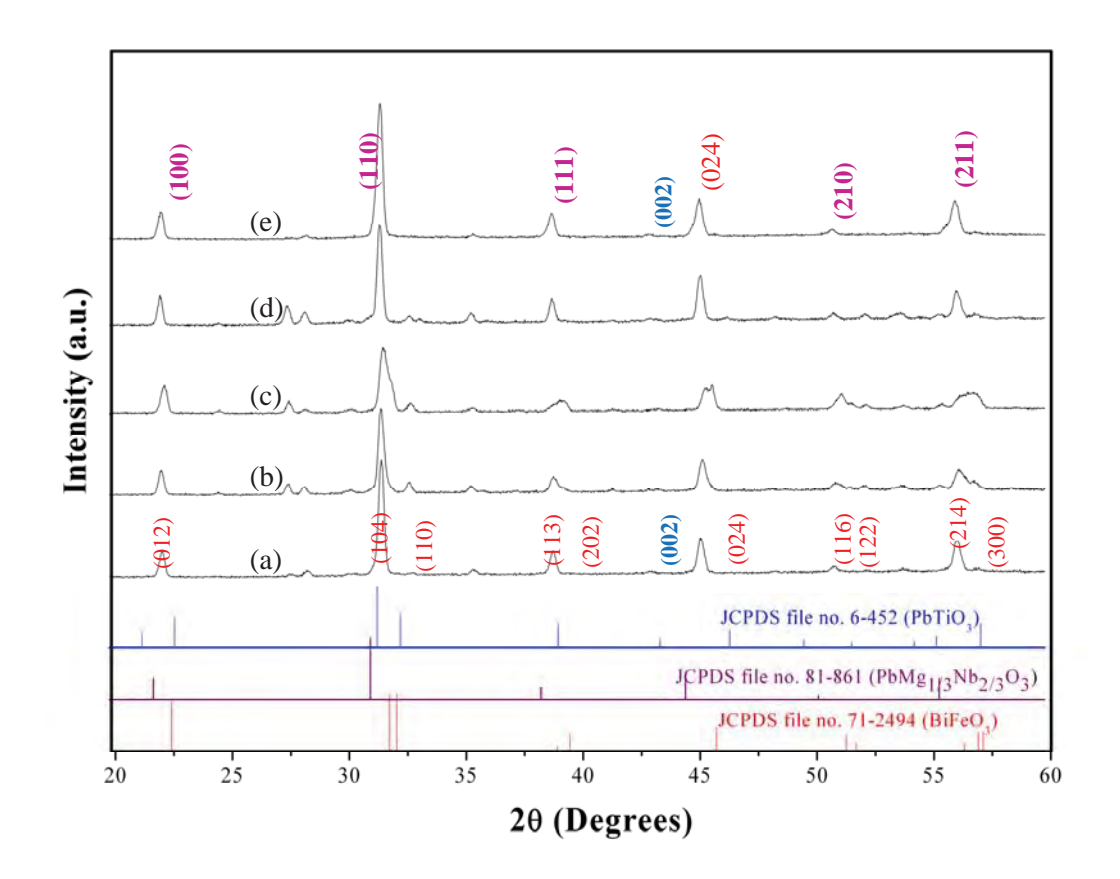


Fig. 1

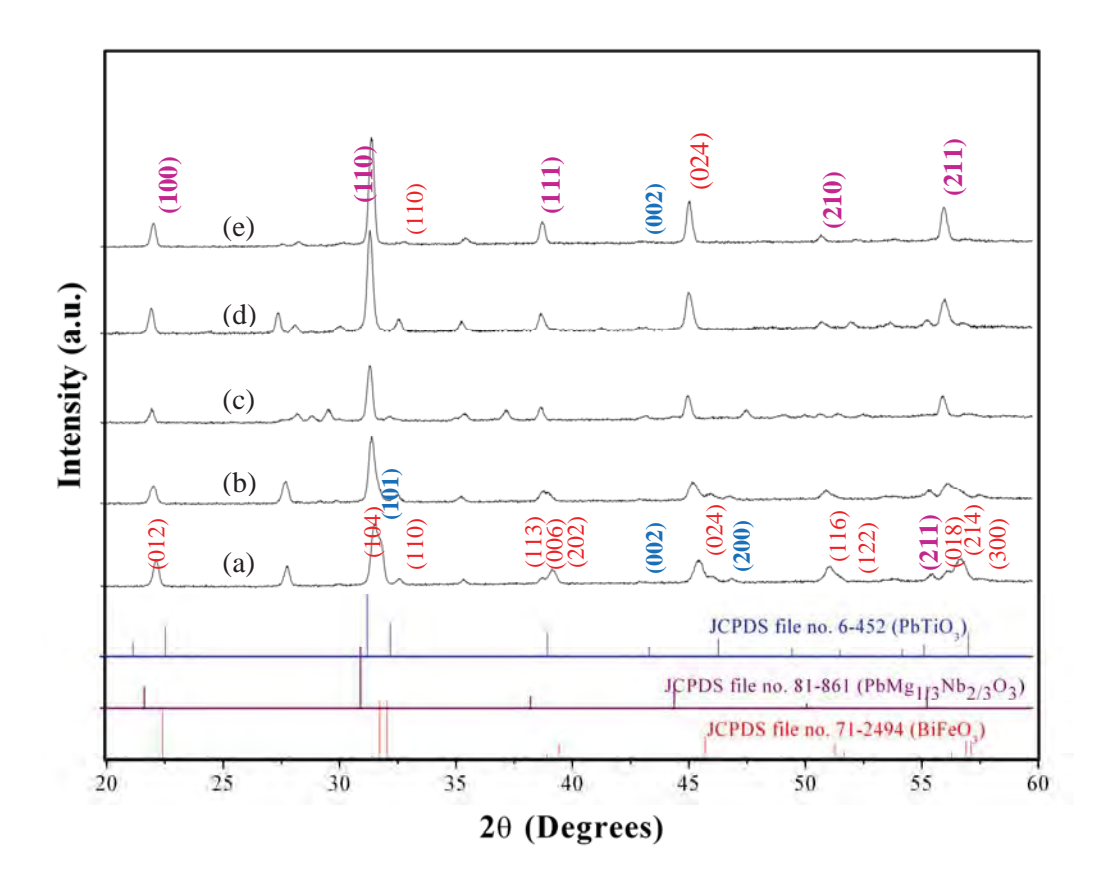
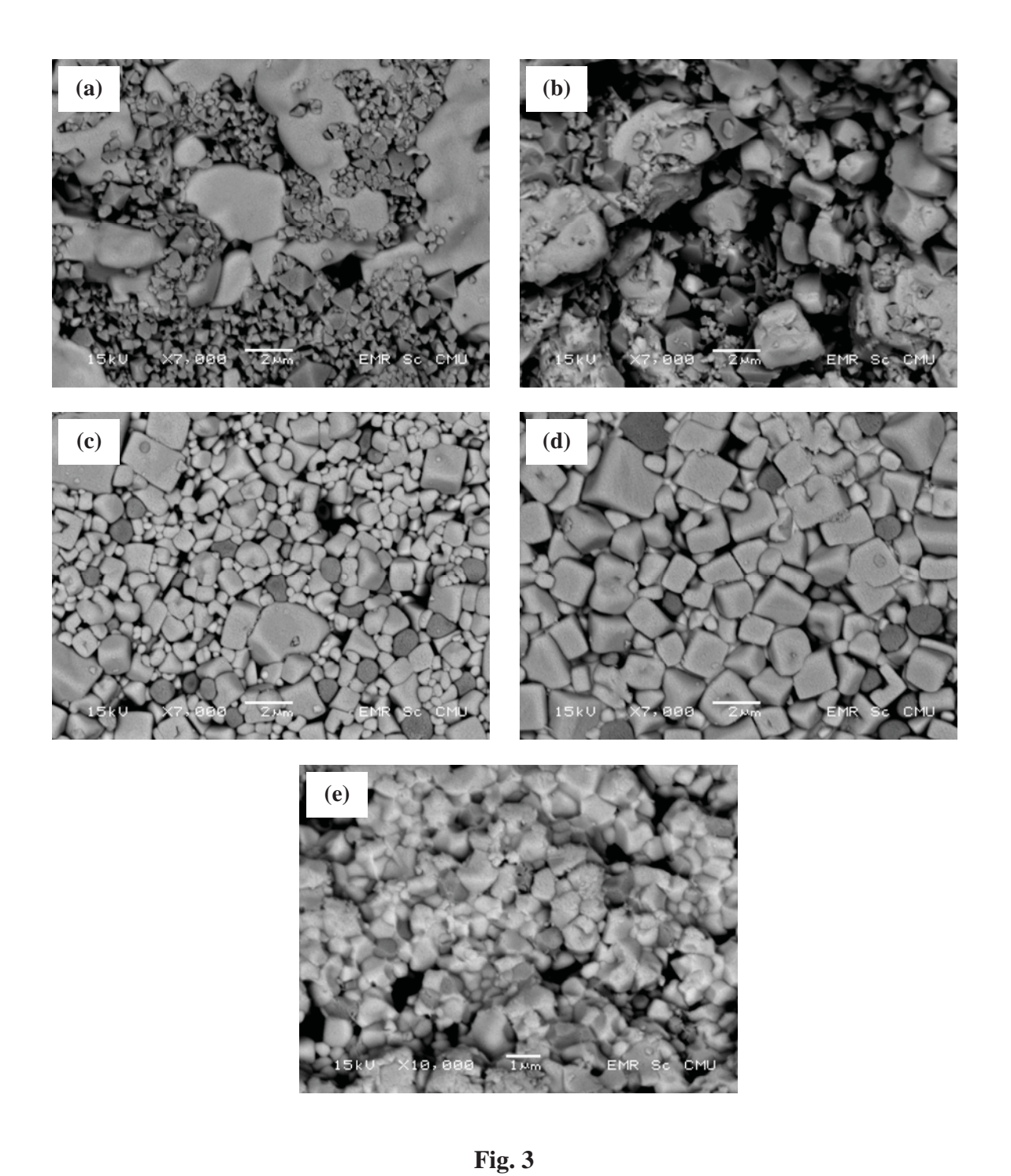


Fig. 2



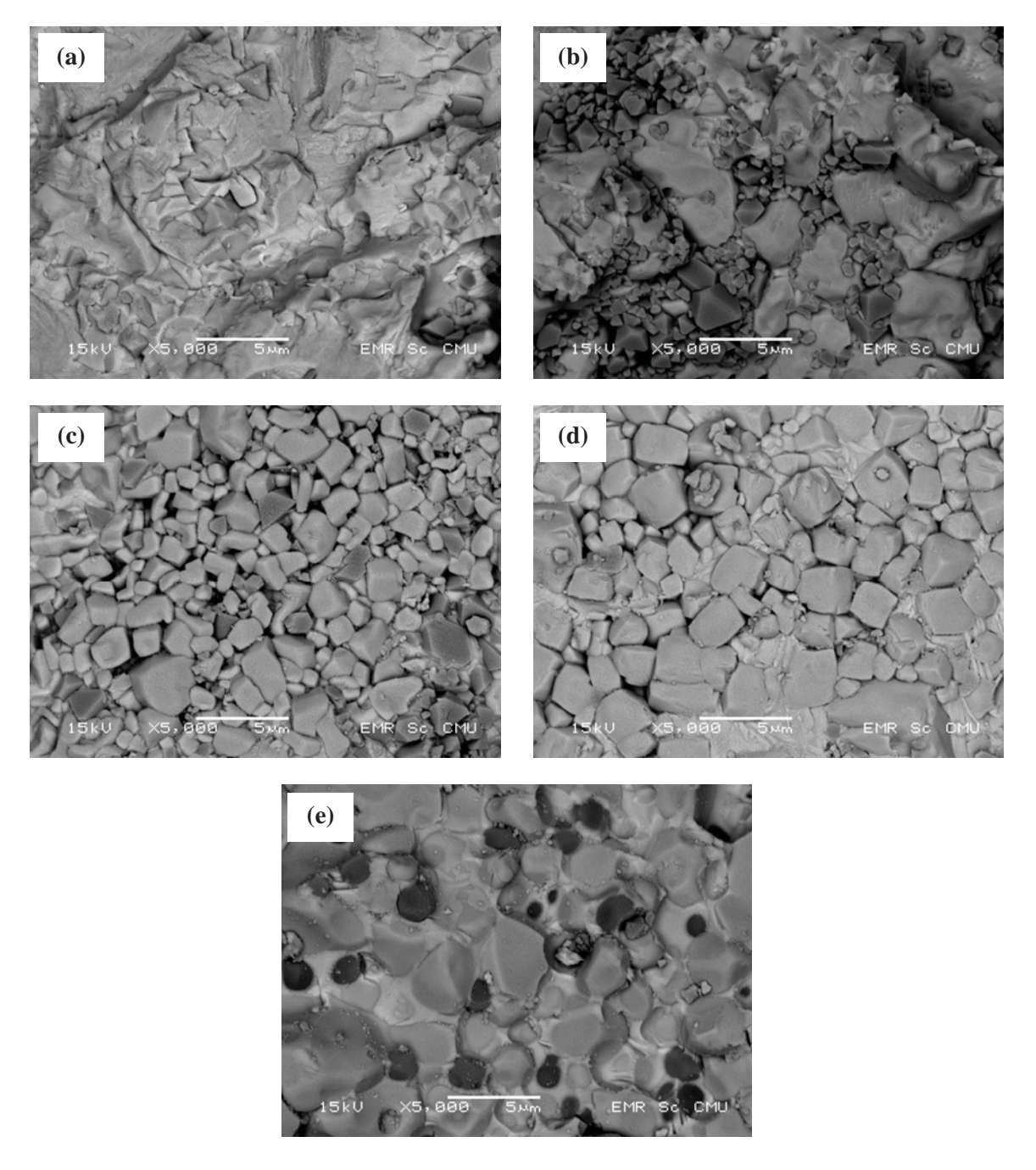


Fig. 4

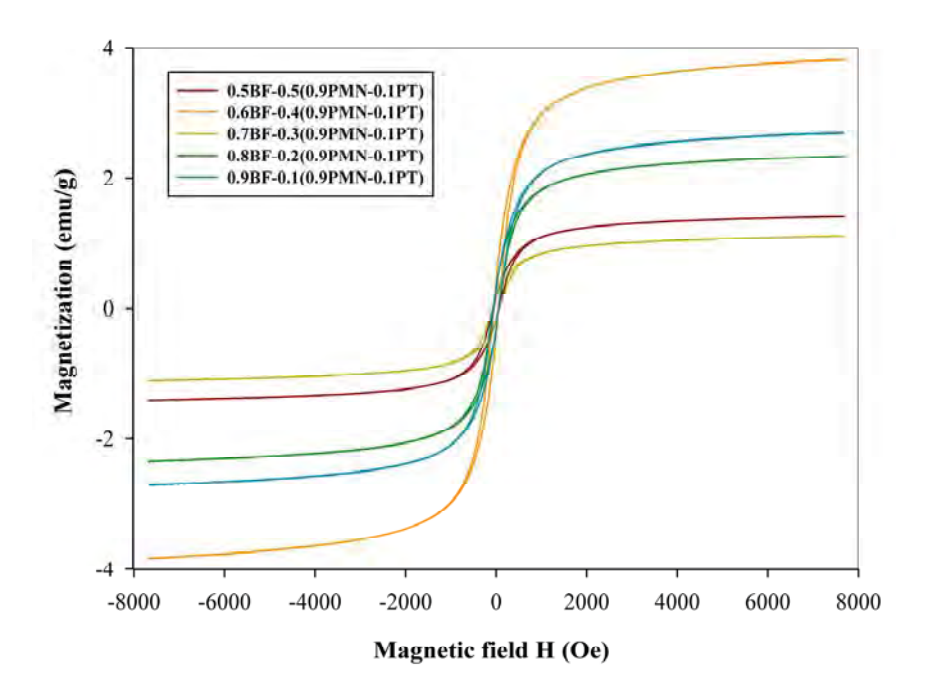


Fig. 5

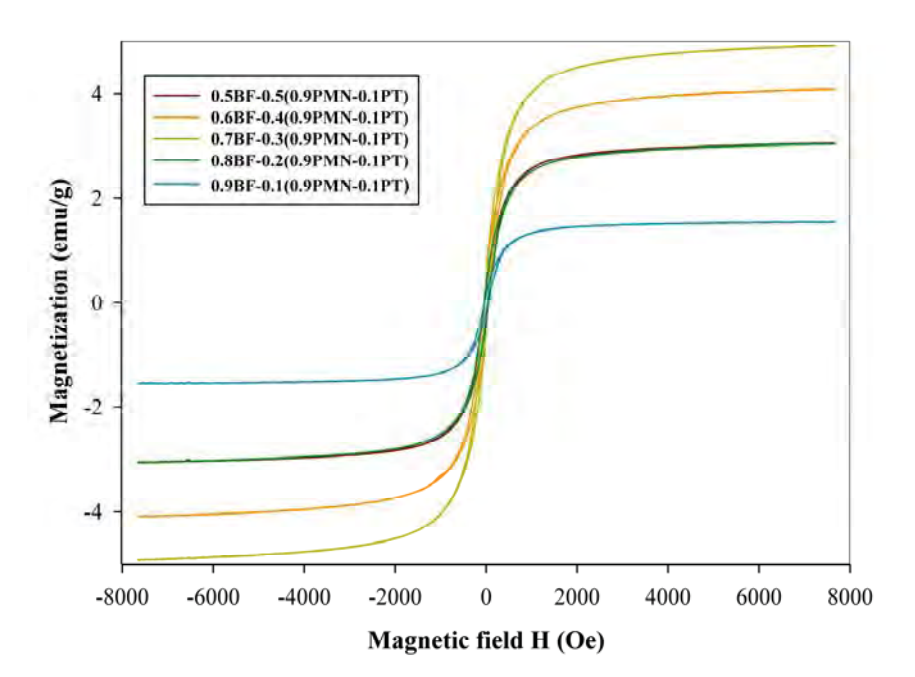


Fig. 6

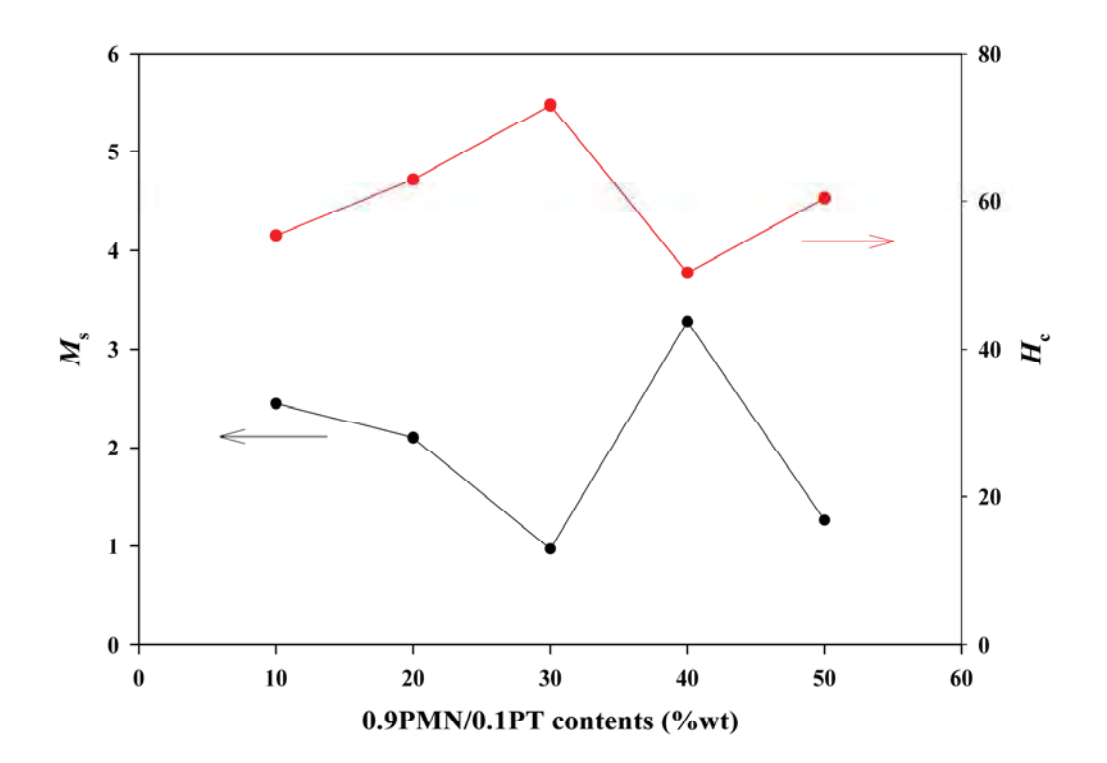


Fig. 7

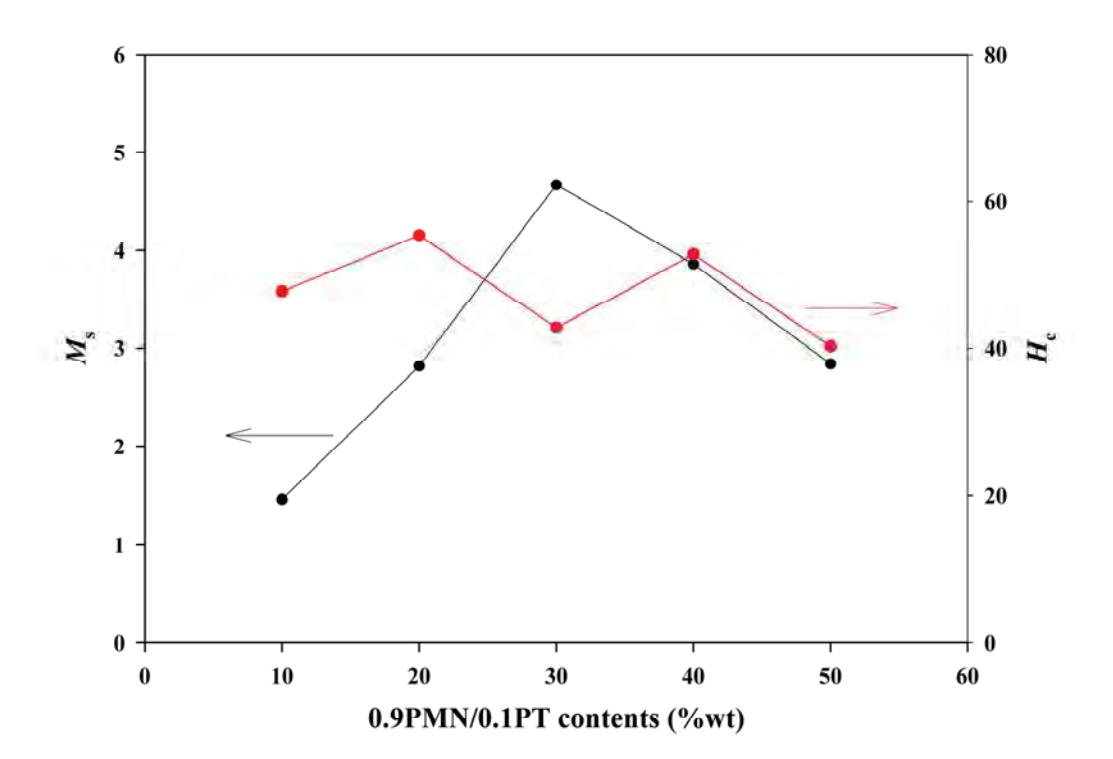
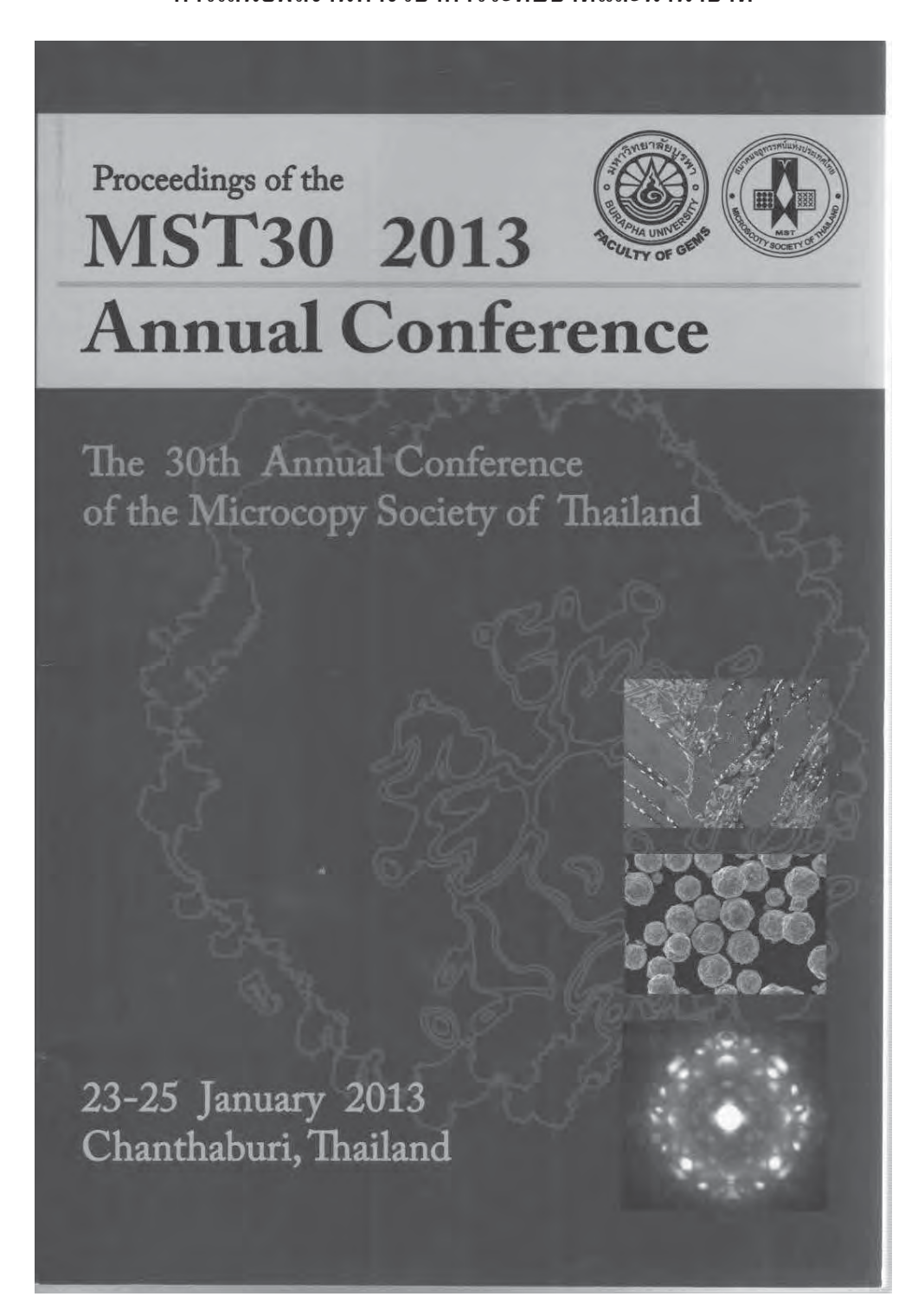


Fig. 8

# การเสนอผลงานทางวิชาการระดับชาติและนานาชาติ



Poster Presentation

## Effect of Milling Time on Phase Formation and Physical Properties of PbFe<sub>1/2</sub>Ta<sub>1/2</sub>O<sub>3</sub>

Thanakrit Kannasut and Rewadee Wongmaneerung\*
Materials Science program, Faculty of Science, Maejo University, Chiang Mai, Thailand
\*Corresponding author, e-mail: re\_nok@yahoo.com

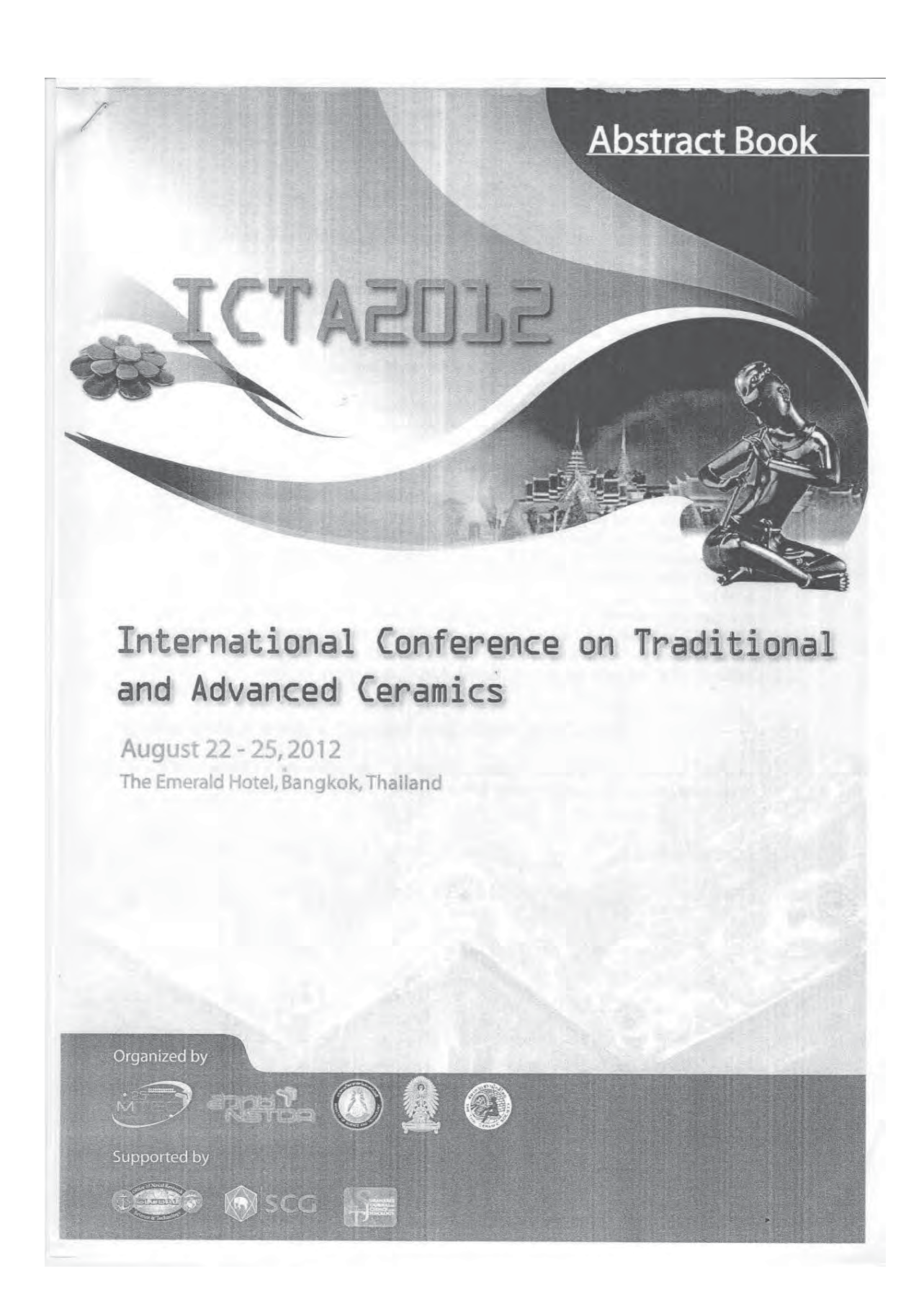
Abstract
Lead iron tantalite (PbFe<sub>1/2</sub>Ta<sub>1/2</sub>O<sub>3</sub> or PFT) is a member of multiferroic materials which exhibiting more than one ferroic order parameter and have potential for applications as actuators, switches, magnetic field sensors or new types of electronic memory devices. PFT has a disordered perovskite-type structure and exhibits the diffuse paraelectric—ferroelectric transition at about ~30 °C [1]. Moreover, PFT belongs to a group of relaxors difficult to synthesize. To fabricate them, a fine powder with a minimal degree of particle agglomeration is needed as the starting material in order to achieve a dense and uniform microstructure at a given sintering temperature. In order to improve the sintering behaviour of PT ceramics, a crucial focus of powder synthesis in recent years has been the formation of uniform-sized, single morphology particulates ranging in size from nanometer to micrometers [2-4].

micrometers [2-4].

Therefore, in this study, PFT powders were synthesized by Columbite precursor method and solid-stated reaction using ball-milling technique. The effect of milling time on phase formation and particle size of PFT powder was investigated. Conventional ball-milling have been used as milling method, with the formation of the PFT phase investigated as a function of calcinations by DTA/TG and XRD. Morphology, crystal structure and phase composition were determined via SEM and EDS technique. It was found that an average particle size trend to decrease with increasing milling time and high degree of particle agglometation was observed. In addition, pure PFT phase can be successfully achieved for all calcinations temperature.

- J. Kulawik, D. Szwagierczak, Dielectric properties of manganese and cobalt doped lead iron tantalate ceramics, J. Eur. Ceram. Soc. 27, 2281–2286 (2007).
   J.S. Wright, L.F. Francis, Phase development in Si modified sol-gel-derived lead titanate, J. Mater. Res. 8.
- R. Wongmaneerung, T. Sarakonsri, R. Yimnirun, S. Ananta, Effects of milling method and calcination condition on phase and morphology characteristics of Mg<sub>4</sub>Nb<sub>2</sub>O<sub>9</sub> powders, Mater. Sci. Eng. B 130, 246-253 (2006).
- 233 (2000).
  R. Wongmaneerung, R. Yimnirun, S. Ananta, Effect of vibro-milling time on phase formation and particle size of lead titanate nanopowders, Mater. Lett. 60, 1447–1452 (2006).

164



International Conference on Traditional and Advanced Ceramics

#### AP-148

#### Studies on Bismuth Ferrite-Lead Titanate Multiferroic Composites

Multiferroic composites consisting of antiferromagnetic BiFeO<sub>3</sub> (BF) and ferroelectric PbTiO<sub>3</sub> (PT) phase were synthesized by the solid-state sintering method. The presence of pure phase in these composites was confirmed by X-ray diffraction (XRD). The microstructure, dielectric and magnetic properties were investigated by mean of scanning electron microscope (SEM), LCR meter and vibrating sample magnetometer (VSM), respectively. Structural transformation from rhombohedral (x = 0.0) to mix phase between rhombohedral and tetragonal (x = 0.5) has been reveal from XRD analysis. The effect of constituent PT phase variation on dielectric constant and hysteresis loop found to be increase/decrease as the content of PT increase. The study of M-H curve reveals that the composites exhibited superparamagnetic at room temperature for all compositions, unlike that of the earlier reported BF-PT solid-solution.

Keywords: Multiferroic, Composites, BiFeO3-based ceramics, Perovskite

\*Corresponding Author: R. Wongmaneerung, Faculty of Science, Maejo University, Chiang Mai 50290, Thailand and E-mail Address: re nok@yahoo.com



# The 8<sup>th</sup> Asian Meeting on Ferroelectrics (AMF-8)

9-14 December 2012 · Pattaya · Thailand www.slri.or.th/amf8

# **Program and Abstracts Book**



Organized by



electric field, temperature and strain. Currently a variety of theoretical approaches are used to gain a deeper understanding of the influence of extensive variables on the dynamic properties of ferroelectric materials in order to tailor the ferroelectric materials for industrial applications. In this paper a recently developed analytical Landau type model for second order bulk materials is extended to include the effects of strain for studying dynamic ferroelectric behaviour under the combined effect of electric field, temperature and strain. Exact expressions are derived analytically for equilibrium polarization and switching time. The exact expressions will be used to examine the dynamic ferroelectric behaviour in regimes of high electric field and strain. The second aspect of this work is to examine the relationship between empirical rules currently used to describe dynamic behaviour in comparison with the exact expressions derived in this paper where the effects of strain has been included.

\* Corresponding author's e-mail: onglh@usm.my

P2 053

Investigation of dynamic behavior of domain structure in [(Na<sub>0.7</sub>K<sub>0.2</sub>Li<sub>0.1</sub>)<sub>0.5</sub>Bi<sub>0.5</sub>]TiO<sub>3</sub> ceramics

Kunyu Zhao<sup>\*</sup>, Huarong Zeng, Jiangtao Zeng, Senxing Hui, Guorong Li and Qingrui Yin

Key Laboratory of Inorganic Functional Materials and Devices, Shunghai-Institute of Ceramics, Chinese Academy of Science, 1295 Dingxi Road, Shanghai 200050, China

We studied the domain structure of lead-free ceramics  $[(Na_0, K_{0.2}L_{la})_{lo,3}Sh_{0.3}]TiO_3$  by piezoresponse force microscopy (PFM). The typical nano-scale fingerprint-like domain structure was revealed in the ceramics, indicating the relaxor characteristic of the sample. The dynamic response of polar nanodomains to the eternal electric fields was also researched by PFM. The spatial inhomogeneity of switching behavior for polar nanodomains was found and the mechanism for the polarization switching properties was discussed in the paper.

\*Corresponding author's e-mail; zhaokunyu@mail.sic.ac.cn

P2 054

 $\begin{array}{c} Defect \ Chemistry \ and \ Dielectric \ Behavior \ of \\ Ba_{0.6}Sr_{0.4}(Ti_{0.99}Fe_{0.01})O_{3.9-\delta}F_{y} \end{array}$ 

W. Menesklou 1,4, F. Paul 2, J. Binder 3 and E. Ivers-Tiffée 1,4

Institut für Werkstoffe der Elektrotechnik (IWE) Karlsruhe Institute of Technology (KIT), Adenauerring 20h, 76131 Karlsruhe, Germany \*Institute of Microsystems Engineering (IMTEK), University of Freiburg, Georges-Koehler-Allee 102, 79110 Freiburg, Germany

Institute for Applied Materials, Karlsruhe Institute of Technology (KIT), Hermann-van-Helmholtz-Platz I, 76344 Eggenstein-Leopoldskafen, Germany

\*DFG Center for Functional Nanastructures, Karlsruhe Institute of Technology (KIT), 76131 Karlsruhe, Germany

Ba<sub>0.6</sub>Sr<sub>0.4</sub>TiO<sub>3</sub> (BST) is the most promising material for realizing tunable passive microwave components. To further improve the relevant properties a lot of studies have been done on micro structure, crystallinity, strain, lattice defects, etc. particularly, focused on thin films. Less work has been published on the impact of dopants on loss tangent and tunability. Especially, investigations of the impact of donors incorporated on the oxygen sublattice are rare. The impact of fluoride as a donor dopant on loss tangent and tunability of Ba<sub>0.6</sub>Sr<sub>0.4</sub>(Ti<sub>0.09</sub>Fe<sub>0.01</sub>O<sub>5.5,a</sub>F, bulk ceramics has been investigated. The dielectric properties were measured on ceramic capacitor structures at frequencies ranging from 10 Hz to 100 MHz and at temperatures ranging from 10 Hz to 100 MHz and at temperatures ranging from 50 °C to 160 °C. The incorporation of fluoride (y=0...0.01) on oxygen sites is confirmed by measurements of electrical conductivity vs. oxygen partial pressure ( $\rho$ O<sub>2</sub> = 10<sup>-15</sup> - 1 bar) at high temperatures ( $\rho$ O<sub>0</sub> = 0.90°C). From these measurements the amount of incorporated fluorideanions has been evaluated quantitatively using defect modeling. As a result of fluoride doping a significant improvement of tunability without increasing loss tangent can be observed. The impact of fluoride on the dielectric behavior is interpreted with respect to charged defects and their interaction as defect associates.

\*Corresponding author's e-mail: menesklou@kit.edu

P2\_055

Magnetic properties of (1-x)BF-xPMN multiferroic composites

Rewadee Wongmaneerung 1.4, Pongsakorn Jantaratana<sup>2</sup>, Rattikorn Yimnirun 3 and Supon Ananta 4

Faculty of Science, Maejo University, Chiang Mai 50290, Thailand Department of Physics, Kasetsart University, Bangkok 10900, Thailand School of Physics, Institute of Science, Suranaree University of Technology, Nakhon Ratchasima 30000, Thailand Department of Physics and Materials Science, Faculty of Science, Chiang Mai University, Chiang Mai 50200, Thailand

Multiferroic composites consisting of ferrite BiFeO<sub>2</sub> (BF) and relaxor ferroelectric Pb(Mg<sub>1/3</sub>Np<sub>2/2</sub>)O<sub>2</sub> (PM) were synthesized by the mixed oxide route. The phase assemblage, microstructure and magnetic properties of the samples were investigated by X-ray diffraction (XRD), scanning electron microscope (SEM) and vibrating sample magnetometer (VSM), respectively.

The results indicate that the PMN phase is compatible with BF phase. The microstructure display the mix phases between BF, PMN and Fe-rich. Interestingly, the M–H hysteresis loop measurements reveal that these composites exhibited weak ferromagnetic behavior at room temperature and magnetization value was higher than that of BF ceramic. Hence BF-PMN prepared in study can be leads to ferromagnetic state that has remanent magnetization, unlike that of the earlier reported BF.

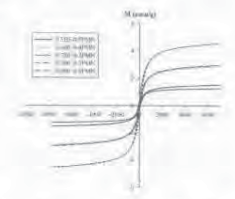


Fig. 1 M–H hysteresis loops of (1–x)BF–xPMN multiferroic composites sintered at 800 °C.

\*Corresponding author's e-mail: re\_nok@yahoo.com

P2 056

Investigations on  $0.1Ni_{0.8}Zn_{0.2}Fe_2O_4$ - $0.9Pb_1$ - $_{3x/2}La_xZr_{0.65}Ti_{0.35}O_3$  composites

Rekha Rani<sup>1</sup>, J.K. Juneja<sup>2</sup>, Chandra Prakash<sup>3</sup> and K.K. Raina<sup>1</sup>

School of Physics & Materials Science, Thapar University, Panala-147004, India

Department of Physics, Hindu College, Sonepat-131001, India

Directorate of ER&IPR, DRDO, DRDO Bhawan, New Delhi-(10105) India

Magnetoelectric materials consisting of both ferromagnetic/ferrimagnetic and ferroelectric phases have been the focus of scientists due to their potential applications in many multifunctional devices such as magnetic field sensors, filters, oscillators, phase shifters, multiple state memory elements, transducers and electro-optic devices etc. The area of magnetoelectric materials has attracted researchers from both groups (Ferroelectricity and Magnetism) because it involves both ferroelectric and magnetic properties of matter. These materials show magnetoelectric (ME) effect which is a coupled two field effect i.e. induced magnetization as a response to an applied electric field or induced polarization by applying an external magnetic field.

Here we are reporting the investigations on composites of nickel zinc ferrite and La substituted lead zirconate titanate with compositional formula  $0.1Ni_{0.8}Zn_{0.2}Fe_2O_4$ - $0.9Pb_{1.5x_0}La_1Zn_{0.2}Ti_{0.3}O_1(x=0.01\ \&\ 0.03)$ . Samples were synthesized by conventional solid state reaction method. The presence of individual phases (ferrite & ferroelectric) was confirmed by X-ray diffraction analysis. SEM micrographs were taken for microstructural study of the samples. Dielectric studies were done as a function of temperature (35-500 °C) at 1, 10 & 100 kHz and function of frequency (100 Hz-1 MHz) at room temperature. To study ferroelectric and magnetic ordering in composite samples, P-E and M-H hysteresis loops were recorded respectively. The variation of ME output as a function of applied de magnetic field was studied. There was a significant improvement in properties of studied composites with La substitution

\*Corresponding author's e-mail: gandhirekhag@gmail.com

P2 057

Magnetic properties of Cu doped Ni-Zn ferrite prepared by hydrothermal method

Xiwei Qi<sup>1\*</sup>, Weiqi Han<sup>2</sup>, Xiaoyan Zhang<sup>1</sup>, Jianquan Qi<sup>1</sup>

School of Resources and Materials. Northeastern University at Quimiangdoo Branch, Qinhuangdoo, 066004, Hebei Province, P. R. China

<sup>2</sup> School of Materials and Metallurgy, Northeastern University, Shenyang, 110819, Liaoning Province, P. R. China

A series of Cu doped Ni-Zn ferrite with the composition of Ni<sub>0.2</sub>Zn<sub>0.8.x</sub>Cu<sub>A</sub>FeyO<sub>4</sub> have been prepared using hydrothermal method, in which x varies as 0, 0.1, 0.2, 0.3 and 0.4. The synthesis temperature and reaction time are carried out at 180 °C and 8 h, respectively. The pure spinel crystal structure can be obtained when the cu content is lower than that of 0.2. When the excess cu is doped, the CuO would exist. The saturate magnetization is increase with the increase of Cu content. For example, for x=0, the saturate magnetization is 125 emu/g; for x=0.2, the saturate magnetization is 230 emu/g. The complex permeability µ' and µ' of Cu doped Ni-Zn ferrite is slightly increased. The cut-off frequency is improved with the increase of Cu content. The grain size is increased with the increase the Cu dopant, indicating that Cu dopant is meaningful for sintering densification and grain growth.

\*Corresponding author's e-mail: xw-qi@163.com

# รางวัลที่ได้รับ





